Phytoplankton competition and coexistence: Intrinsic ecosystem dynamics and impact of vertical mixing

Coralie Perruche, Pascal Rivière, Philippe Pondaven, Xavier J. Carton

Journal of Marine Systems
April 2010, Volume 81, Issues 1-2, Pages 99-111
http://dx.doi.org/10.1016/j.jmarsys.2009.12.006

Phytoplankton competition and coexistence: Intrinsic ecosystem dynamics and impact of vertical mixing

Coralie Perruche[a, *], Pascal Rivière[a], Philippe Pondaven[a] and Xavier Carton[b]

[a] Laboratoire des Sciences de l'Environnement Marin, UMR6539 CNRS-UBO-IRD, Institut Universitaire Européen de la Mer, Place Nicolas Copernic, 29280 Plouzané, France
[b] Laboratoire de Physique des Océans, UMR6523 CNRS-Ifremer-UBO-IRD, Université de Bretagne Occidentale, Avenue Le Gorgeu, 29200 Brest, France

*: Corresponding author : Pascale Lherminier, Tel.: +33 2982 24362; fax: +33 2982 24496, email address : pascale.lherminier@ifremer.fr

Abstract:

This paper aims at studying analytically the functioning of a very simple ecosystem model with two phytoplankton species. First, using the dynamical system theory, we determine its nonlinear equilibria, their stability and characteristic timescales with a focus on phytoplankton competition. Particular attention is paid to the model sensitivity to parameter change. Then, the influence of vertical mixing and sinking of detritus on the vertically-distributed ecosystem model is investigated.

The analytical results reveal a high diversity of ecosystem structures with fixed points and limit cycles that are mainly sensitive to variations of light intensity and total amount of nitrogen matter. The sensitivity to other parameters such as re-mineralisation, growth and grazing rates is also specified. Besides, the equilibrium analysis shows a complete segregation of the two phytoplankton species in the whole parameter space.

The embedding of our ecosystem model into a one-dimensional numerical model with diffusion turns out to allow coexistence between phytoplankton species, providing a possible solution to the 'paradox of plankton' in the sense that it prevents the competitive exclusion of one phytoplankton species. These results improve our knowledge of the factors that control the structure and functioning of plankton communities.

Keywords: Modelling; Ecosystem; Competition; Phytoplankton; Dynamical system; Water mixing

1 Introduction

Plankton biodiversity has always intrigued biologists who wondered how it was possible that numerous phytoplankton species can coexist on a very limited number of mineral resources (the "paradox of plankton" described by Hutchinson (1961)). A few explanations have been given to this paradox (see for a review, Roy and Chattopadhyay, 2007): predator control (Krivan, 1996, 1997), temporal forcing such as the seasonal cycle (Hutchinson, 1961), spatio-temporal effects (ocean dynamics) which will interest us in the present study, and self-organized ecosystem dynamics (Huisman and Weissing, 1999; Passarge and Huisman, 2002).

Numerous sea surveys have been conducted to answer this paradox and two methods were successively used to extract data on phytoplankton diversity: cell counts (Riley, 1957; Jeffrey and Hallegraeff, 1980; Fryxell et al., 1985) and the measurement of photosynthetic pigments used as biomarkers (Claustre et al., 1994; Vidussi et al., 2001; Vaillancourt et al., 2003; Sweeney et al., 2003; Dandonneau et al., 2006). These studies revealed that the distribution of phytoplankton species or size class was related to dynamical structures such as cyclones, anticyclones, fronts. This showed a clear connection between the dominating species and ocean dynamics, which constrains the distribution of nutrients and light available for the plant. But these data are really difficult to interpret because they result from many possible phenomena; furthermore, they did not provide an adequate sampling to resolve the spatio-temporal biological variability.

Modelling is a way to describe interactions inside an ecosytem, which can then be embedded in a simulated ocean circulation to study its behaviour in

a pelagic environment. Bracco et al. (2000) showed a slowdown of the weak species disappearance in a highly turbulent circulation. Rivière and Pondaven (2006), Lima et al. (2002a), Martin et al. (2001) examined the biological response to a fully-developped frontal dynamics using more or less complex ecosystem model, respectively, NPPZD, NPPZZD, and an even more complex model with bacteria and nitrate-ammonium differentiation. They all concluded to a distribution of their two phytoplankton species strongly influenced by mesoscale processes but they had no clear results about what dynamical processes drove their distribution, their coexistence or segregation or if these distributions were intrinsic to the biological system itself. Furthermore, the dependence of conclusions on biological parameters of the ecosystem was unknown. Anderson (2005), for instance, raises the question of the accuracy of results given by complex ecosystem models when the system dynamics and parameterisation sensitivity are not well known.

All these results motivate the following general question : Do ocean dynamics, via advection and diffusion, affect the ecosystem structure especially with respect to phytoplankton competition on a limited number of resources? To address such a question, models are ideal tools; indeed, they allow a study of dominant mechanisms, from ecosystem functioning to ocean dynamics. In the present study we choose to focus on the effects of particular dynamical process, vertical diffusion, on phytoplankton competition. Our strategy is as follows: first gain knowledge of the intrinsic dynamics of a simple ecosystem model (0D model) by means of an analytical study, and then use these results to understand the effects of vertical diffusion on phytoplankton competition.

Up to now, simple ecosystem models with one phytoplanlton species were studied analytically. Franks et al. (1986) determined the equilibria of an NPZ

model (Wroblewski and O'Brien, 1976) and the sensitivity of equilibrium values to biological parameters and especially to phytoplankton growth rate. Busenberg et al. (1990), with the same model, made a more detailed analytical study with rigorous calculations of equilibria and their linear stability as a function of biological parameters. The studies of Edwards and Brindley (1999) and Edwards (2001) also used analytical and numerical techniques to determine the dynamical behaviour of their ecosystem and concentrated on sensitivity to ecosystem parameters and in particular to zooplankton mortality with NPZ and NPZD models of different complexity. The question of competition dynamics between phytoplankton species within an ecosystem model was addressed by Lima et al. (2002b). However their results were obtained numerically through integration of model equations using Runge-Kutta method. This approach is too expensive to allow a study of model parameter sensitivity. Besides, it does not give characteristic time scales of the model independent of initial conditions. In the present study we choose to use a model of intermediate level of complexity (NPPZD) to address the question of marine ecosystem structuring in an analytical way. Our model, though simple, allows the investigation of phytoplankton competition within an ecosystem.

Hereafter we first describe our ecosystem model: equations and parameters. This provides its domain of use and limits. With the mathematical tools of dynamical systems, we determine the different equilibria (fixed points and limit cycles), the transitions between them in the parameter space and the intrinsic time scales associated with each equilibrium. Then we examine the ecosystem model sensitivity to parameters with a particular focus on the influence of light and total amount of nutrient stock (particulate and dissolved). After, the ecosystem model is embedded in a one-dimensional physical model to determine the role of vertical diffusion and sedimentation on phytoplankton

competition. Finally, we discuss these results with a focus on ecosystem time scales and their possible interactions with vertical diffusion and more generally with ocean dynamics.

2 Description of the ecosystem model

The ecosystem model used here has 5 prognostic variables: N, P_1, P_2, Z, D which are respectively nutrients, small phytoplankton, large phytoplankton like diatoms, zooplankton, and detritus. This model is based on the structure of classical NPZD models like those of Fasham et al. (1990), Denman and Pena (1999), Busenberg et al. (1990), Lima et al. (2002b) and Olson and Hood (1994). The first two models were used to study the seasonal cycle of plankton dynamics in the oceanic mixed layer. The two following ones were used to study the ecosystem structuring in the parameter space. The last one has the simplest equations, which allow to calculate the equilibrium solutions. Then, Olson and Hood (1994) coupled it with a one-dimensional dynamical model and showed that idealised seasonal forcings can slow down the competitive exclusion of one of the two phytoplankton species. Here, our model has an intermediate level of complexity. The modelled ecosystem is aimed at a pelagic environment. Only the autotroph level has two variables and therefore, it allows to study phytoplankton competition. For seek of simplicity, we consider nitrogen as the limiting element, acknowledging the fact that other elements like phosphorus, silicon or iron can limit phytoplankton growth. The ecosystem structure is outlined in Fig. 1. In this model each variable is quantified by its equivalent scalar nitrogen concentration ($mmol\ N.m^{-3}$).

The non-linear model equations are :

$$\frac{dN}{dt} = \tau D - \alpha_1 \frac{N}{K_{N1} + N} P_1 - \alpha_2 \frac{N}{K_{N2} + N} P_2 \tag{1}$$

$$\frac{dP_1}{dt} = \left(\alpha_1 \frac{N}{K_{N1} + N} - m_p \right) P_1 - g \frac{P_1}{K_Z + P_1 + P_2} Z \tag{2}$$

$$\frac{dP_2}{dt} = \left(\alpha_2 \frac{N}{K_{N2} + N} - m_p \right) P_2 - g \frac{P_2}{K_Z + P_1 + P_2} Z \tag{3}$$

$$\frac{dZ}{dt} = \left[g\beta \frac{P_1 + P_2}{K_Z + P_1 + P_2} - \varepsilon \right] Z \tag{4}$$

$$\frac{dD}{dt} = \left[g(1-\beta) \frac{P_1 + P_2}{K_Z + P_1 + P_2} \right] Z + m_p (P_1 + P_2) + \varepsilon Z - \tau D \tag{5}$$

with $\alpha_1 = \mu_1(1 - exp(\frac{-I}{K_{I1}}))$ et $\alpha_2 = \mu_2(1 - exp(\frac{-I}{K_{I2}}))$.

Definitions and values of the parameters are given in Table 1. The sum of these equations is null so the total amount of nitrogen, C_0, is conserved : $N + P_1 + P_2 + Z + D = C_0$. We chose a closed system and not a chemostat because it is aimed at being embedded in a vertical model with nutrient fluxes due to physics. In addition, it is more easily studied analytically. Each term of these equations is a flux between two variables and is represented by an arrow in Fig. 1. Phytoplankton growth is controlled by light (I) and nutrient concentration (N) in the tank. The growth rate consists in 3 factors: μ_i, the maximum growth rate (unit: day^{-1}), the Michaelis-Menten function that parameterizes the nutrient limitation (dimensionless values comprised between 0 and 1) and the light limitation (dimensionless values comprised between 0 and 1). This growth rate is multiplied by the phytoplankton concentration to obtain the term of nutrient uptake in the phytoplankton equations 2 and 3. The terms responsible for the decline of phytoplankton in equations 2 and 3 are respectively natural mortality and grazing. The formulation for the two phytoplankton species is the same, P_1 and P_2 are only differentiated by their

maximal growth rate (μ_i), their affinity for either nutrients ($K_{N\,i}$) or light ($K_{I\,i}$).

Parameters vary according to species that are described in the ecosystem model. Their range of variations must be defined to study model parameter sensitivity. Upper and lower limits for maximal growth rates can be constrained using allometric laws. Maximal growth rates (μ_i) at 20°C range from $\sim$0.2 day^{-1} to 3 day^{-1} (see for example Banse, 1982; Moloney and Field., 1989). In open ocean phytoplankton communities, $K_{N\,i}$ is usually $<$ 1 $mmol\ N.m^{-3}$ for nitrates (Harrison et al., 1996). We derive range of $K_{I\,i}$ using data from Taguchi (1976) who studied the relationship between photosynthesis and cell size in marine diatoms. The range for $K_{I\,i}$ varies from 2 to 50 $W.m^{-2}$. Finally phytoplankton natural mortality (m_p), our default value of 0.045 day^{-1} is in the range reported by Fasham et al. (1990) (modelling study) and by Marbà et al. (2007) and Agustí et al. (1998) (estimates of phytoplankton lysis).

In our model, a single zooplankton variable represents a herbivorous microzooplankton. Its mass balance is governed by a growth term minus a mortality term. The growth term is described by a Michaelis-Menten functional response which depends on the maximal ingestion rate, g, and the half saturation constant for ingestion, K_Z. In addition, part of the ingested food is not transformed into biomass. In the model, this is taken into account with the gross growth efficiency parameter, β, which is the ingested part of the grazed phytoplankton after losses by excretion and fecal pellets. Finally, a linear loss term (εZ) is used to represent natural mortality. It is a 'closure term' which represents the consumption of zooplankton by higher predators. We consider here a linear formulation for zooplankton natural mortality as was done by

Fasham et al. (1990), Busenberg et al. (1990) and Edwards and Brindley (1999). Its value is equal or very close to the values of these three studies. We chose a linear term instead of a quadratic one because we checked that it did not change fundamentally our ecosystem dynamics in contrast to the results of Steele and Henderson (1992). Indeed, we have similar results to those of Edwards and Brindley (1999) with oscillations occuring across broader ranges of parameters in linear than in quadratic formulation. In order to be able to lead the analytical study as far as possible, we chose the linear term.

Ranges for ingestion rates and half saturation constants for ingestion were calculated according to Moloney and Field (1991), g varies from 6.30 day^{-1} to 0.35 day^{-1} for predator size ranging from 10^4 to 10^9 $pg\ C$, and K_Z varies from 0.46 to 3.56 $mmol\ N.m^{-3}$ for prey size ranging from 10^{-2} to 10^9 $pg\ C$. For β, the gross growth efficiency, Straile (1997) has shown that it is not that different between protists and copepods with a global average of about 20-30 %. Mortality rates also scale with size across a large size spectrum from protists to whales (McGurk, 1986). For microzooplankton or young stages of copepods, Kiørboe (1997) found that mortality rates range from 0.02 to 0.5 day^{-1}, with most values < 0.2 day^{-1}. For adult copepods, average daily mortality rates (ε) are around $\sim$0.1 day^{-1} (Hirst and Kiørboe, 2002).

The detritus concentration in equation 5 increases with the non-assimilated part of grazing along with the dead organisms. It decreases through remineralisation which transforms detritus into nutrients. Finally, the tank of nutrients in equation 1 is fed by detritus remineralisation and is emptied by phytoplankton uptake. Specific degradation of organic matter ranges from 0.003 day^{-1} to 0.44 day^{-1} at temperature ranging from 5 to 26°C (Newell et al., 1981; Biddanda and Pomeroy, 1988; Panagiotopoulos et al., 2002; Lønborg, 2009).

Here, the detritus remineralisation rate is set to 0.1 day^{-1} like Edwards (2001).

Each flux between two ecosystem variables is associated with one time scale, which is defined by parameters. But the difficulty is to deduce a global characteristic time scale from the combination of the whole set of parameters, which would quantify the ability of the system to adapt to a new environment and the rate at which it reacts. The mathematical tools of dynamical system theory, described in the next section, will allow us to determine such a time scale as a function of parameters.

The two phytoplankton species (see Table 1) have different preferences for nutrients and light, two essential ingredients for photosynthesis. In the open ocean, small phytoplankton species are rather encountered in nutrient-limited environments. On the contrary, large species are rather adapted to conditions propitious to blooms. Here, P_1 represents a picophytoplankton-like (e.g small flagellates) better adapted to low-nutrient and high-light conditions while P_2 represents a nano- or micro-phytoplankton-like (for example diatoms) better adapted to high-nutrient and low-light conditions (Margalef, 1958). So the sea surface conditions better suit P_1, and P_2 is better adapted to conditions characteristic of subsurface. Indeed Fig. 2 shows the ratio between P_2 and P_1 growth rates as a function of light I and nutrients N. P_1 is actually stronger (ratio lower than one) with rather high light intensity whereas P_2 is dominant in low-light conditions.

This model is a simplified version of that used by Rivière and Pondaven (2006). Our goal was to find a compromise between simplicity and realism to be able to study the 0D model analytically. For this purpose, we modified the zooplankton growth term by considering only the grazing of the two phytoplank-

ton species with fixed preferences. In this study, we want to focus on the bottom-up control of the phytoplankton species concentration by nutrients, so we consider a single zooplankton species that has a mean effect on the two phytoplankton species. It grazes as much P_1 as P_2 (same preference for the two species). The main difference with the original model of Rivière and Pondaven (2006) is that the two phytoplankton species can not coexist anymore in homogeneous conditions (without physics). They are segregated in the whole parameter space as it will be shown in the following section.

3 Intrinsic Ecosystem dynamics

The ecosystem model under focus here is a nonlinear system with 5 equations and 5 variables (equations 1 to 5). Because the system is closed it can be reduced to 4 equations and 4 variables using the relation $D = C_0 - N - P_1 - P_2 - Z$, so that the system becomes:

$$\frac{dN}{dt} = \tau(C_0 - N - P_1 - P_2 - Z) - \alpha_1 \frac{N}{K_{N1} + N} P_1 - \alpha_2 \frac{N}{K_{N2} + N} P_2 \quad (6)$$

$$\frac{dP_1}{dt} = \left(\alpha_1 \frac{N}{K_{N1} + N} - m_p \right) P_1 - g \frac{P_1}{K_Z + P_1 + P_2} Z \quad (7)$$

$$\frac{dP_2}{dt} = \left(\alpha_2 \frac{N}{K_{N2} + N} - m_p \right) P_2 - g \frac{P_2}{K_Z + P_1 + P_2} Z \quad (8)$$

$$\frac{dZ}{dt} = \left[g\beta \frac{P_1 + P_2}{K_Z + P_1 + P_2} - \varepsilon \right] Z \quad (9)$$

This model is a general dynamical system : $\frac{dX}{dt} = f(X, \nu)$ where $X = (N, P_1, P_2, Z)$ and $\nu = (I, C_0, \tau, \mu_1, \mu_2, K_{I1}, K_{I2}, K_{N1}, K_{N2}, m_p, g, K_Z, \varepsilon, \beta)$ are respectively the state variable vector and the parameter vector. All components of X and ν are positive.

Among the parameters of this model, I and C_0 can be classified apart. Indeed, C_0 and I vary artificially in this ecosystem model but vary in space and time in reality. Thus a detailed study of the state vector variations with C_0 and I in 0D is essential to better explain the 3D observations from the sea surface where light is intense to the subsurface where nutrients are abundant.

Now we will first characterize the equilibria of this model and their stability, and then a sensitivity study of the ecosystem model dynamics will be conducted to extract the role of key parameters.

3.1 Equilibrium solutions and their stability

The purpose is to characterize analytically the equilibria and their stability for this dynamical system in the whole parameter space defined by ν. In other words, we are looking for the asymptotic behaviour of the system as $t \to \infty$. The ecosystem structures corresponding to equilibria of the system are listed in Table 2. Two types of equilibrium can be reached by the system : steady equilibria (fixed points) and oscillatory regimes (limit cycles). In our case, there are five possible fixed points with different ecosystem structures and two possible limit cycles (see Table 2). Ecosystems n° 6 and n° 7, which involve phytoplankton coexistence, can not be achieved in such a model. All the analytical determination of the domain of validity of fixed points, bifurcation curves and intrinsic time scales are detailed in Appendix A. The question of phytoplankton coexistence or segregation is dealt with, in Appendix B.

The main conclusion from this analytical study is: whatever the parameter values, the two phytoplankton species can not coexist in our model at equilibrium: one of them is always excluded from the system. Without zooplank-

ton this result is a consequence of the competitive exclusion principle. With zooplankton this result can be interpreted as a consequence of the fixed preferences applied to the phytoplankton. Indeed, if one species is favoured and develops much more than the other, zooplankton does not take into account this dominance and still grazes the same proportion of each species. Zooplankton does not control the species in excessive number and does not spare the other. As we aim to study the effect of diffusion on phytoplankton competition, this model choice is important: it is the most unfavourable case for the two phytoplanktons to coexist.

3.2 Equilibria and associated time scales as a function of light (I) and total nitrogen (C_0)

With the dynamical system theory, we explored analytically the ecosystem equilibria in the whole parameter space. Here, we study the ecosystem structure at equilibrium and the associated time scales as a function of light (I) and total nitrogen (C_0), the other parameters being set to their default value (Table 2). These two parameters have a large range of variation in ocean. At first order, they only vary along the vertical, light is decreasing with depth while nutrient concentration is usually increasing down to the nitracline. Nevertheless they also vary horizontally through combined advection and diffusion processes for nutrients and, through shading due to phytoplankton for light. In that sense the possible values for I and C_0 define a 2D parameter space in which the ecosystem can achieve different equilibria. Our 0D study will provide preliminary and indicative information for the 1D model to follow.

Fig. 3 sums up the different equilibrium solutions on a bifurcation diagram

as a function of I and C_0. As expected, varying parameters I and C_0 causes deep changes in stability of equilibrium solutions. Two types of bifurcation are observed on this diagram: transcritical bifurcations (solid lines on Fig. 3) and Hopf bifurcations (dashed lines on Fig. 3). Fixed points are white areas whereas limit cycles are grey areas on Fig. 3. Each equilibrium is indicated by the emergent variables. Fig. 4 gives the amplitude of each variable at fixed points in the same parameter space. These figures illustrate the main results obtained by the analytical study. First, phytoplankton species do not coexist. P_1 survives for high values of I and P_2 for low values of I. Therefore, P_1 is expected to dominate in surface layers and P_2 in subsurface. Secondly, no zooplankton is observed for low values of C_0. Thirdly, as soon as the zooplankton emerges, concentration of the subsisting phytoplankton remains constant, illustrating zooplankton control of phytoplankton which implies an increase of zooplankton concentration as total nitrogen (C_0) or light (I) increases. Edwards and Brindley (1999) had the same feature in their model with linear zooplankton mortality. Lastly, large values of total nitrogen lead to self-sustained oscillations between nutrient, subsisting phytoplankton and zooplankton. These oscillations occur for parameter ranges corresponding closely to subsurface chlorophyll maximum in the ocean. This kind of oscillations have already been observed with an ecosystem model by Lima et al. (2002b). As a global view of the (I, C_0) bifurcation diagram, we can conclude that phytoplankton emergence is mainly managed by I whereas zooplankton emergence and temporal behaviour is mainly managed by C_0.

With the analytical study, time scales associated with each fixed point can be calculated as a function of light and amount of nutrients (Fig. 5). As expected, there are some differences between time scales associated with conditions of surface and of subsurface. At high light - low nutrient conditions often en-

countered in surface layers, time scales to reach equilibrium range from 1 to 5 days which is quite fast. The ecosystem is very reactive at sea surface. At low light - high nutrient conditions characteristic of subsurface layers, time scales are an order higher ($10-20$ days) and the ecological system is likely to undergo self-sustained oscillations with periods of about 50 days (not shown).

This shows that ecosystem time scales will be very different from the surface to the deep ocean. Ocean dynamics is expected to play an important role on 3D ecosystem structuring through parameters I and C_0, and it is likely to interact with ecosystem dynamics through the coupling of their time scales as it will be dealt with in the discussion.

3.3 Influence of biological parameters on the (I, C_0) equilibrium solutions

After studying the influence of external parameters (I, C_0) on ecosystem structuring, we investigate in the sensitivity of the system to biological parameters.

3.3.1 Sensitivity to the re-mineralisation rate τ

In the real ocean, re-mineralisation associated with sinking is an important process in subsurface chlorophyll maximum dynamics. In our system, re-mineralisation time scale can be thought of as a time scale related to the system closure. This time scale is supposed to be important in our model concerning the competition process between the two phytoplankton species.

Let us consider the effects of varying re-mineralisation parameter τ from 10^{-3} to 1 day^{-1}, for a fixed light intensity of $I = 5\ W.m^{-2}$ but two different total nitrogen concentrations : $C_0 = 1.2\ mmol\ N.m^{-3}$ and $C_0 = 4\ mmol\ N.m^{-3}$

(Fig. 6).

For $C_0 = 1.2\ mmol\ N.m^{-3}$ the system was reaching a fixed point of type $N^*P_2^*Z^*$ with default value of $\tau = 0.1\ day^{-1}$ (Fig. 3). On Fig. 6a, we observe that as τ increases from this value, no more bifurcation is observed, only the amplitude of N and Z increases. As τ decreases from its default value, two consecutive bifurcations are observed: first a new fixed point is achieved with a shift from P_2 to P_1 giving an $N^*P_1^*Z^*$ equilibrium and then another fixed point appears for very low τ values in which zooplankton disappears giving an $N^*P_1^*$ equilibrium. The shift from P_2 to P_1 as τ decreases can be explained as follows: for low re-mineralisation rates the process of re-mineralisation from detritus to nutrients is very slow inducing a drop in nutrient stocks at the equilibrium which is more favourable to small phytoplankton P_1. When τ tends to 0, the $N^*P_1^*$ fixed point remains stable according to eigenvalues λ_1 and λ_2 calculated in the preceding section which remain negative, and N remains constant whereas P_1 decreases towards 0 according to equations A.1 and A.2. In that case re-mineralisation is so slow that it can not balance uptake and thus, at equilibrium, detritus concentration increases while P_1 concentration decreases.

Fig. 6b shows the case in which C_0 is increased to 4 $mmol\ Nm^{-3}$. For the default τ value (Fig. 3) the equilibrium was a limit cycle between N, P_2 and Z. As τ is increased from this default value, this equilibrium remains stable but the amplitude of oscillations increases. Inversely as τ is decreased the periodic orbit collapses and the system reaches an $N^*P_2^*Z^*$ fixed point. Then as τ decreases we observe two more bifurcations similar to the ones observed in Fig. 6a with first a shift from P_2 to P_1 and then disappearance of Z giving an $N^*P_1^*$ fixed point for very low values of τ.

In conclusion, the increase of τ tends to destabilize the system giving rise to oscillations when total nitrogen concentration is sufficient. Large values of τ are favourable to a dominance of P_2, whereas low τ values are favourable to a dominance of P_1. Moreover large values of τ tend to increase biodiversity giving rise to a coexistence of phytoplankton and zooplankton. If we refer to the (I,C_0) bifurcation diagram of Fig. 3 we checked in the analytical study (see Appendix A) that an increase of τ values has no influence on bifurcation lines $N^* \leftrightarrow N^*P_1^*$, $N^* \leftrightarrow N^*P_2^*$ and $N^*P_1^* \leftrightarrow N^*P_2^*$, whereas it tends to translate downwards all the remaining bifurcation curves. It is able to influence phytoplankton competition mainly for medium light values, corresponding to neighborhood of the bifurcation lines $N^*P_1^*Z^* \leftrightarrow N^*P_2^*Z^*$ and $NP_1Z \leftrightarrow NP_2Z$ (limit cycles).

3.3.2 Sensitivity to growth rates μ_1 and μ_2

The sensitivity of the model to the growth rates μ_1 and μ_2 is illustrated on the bifurcation diagram of Fig. 7 in which I is set to 5 $W.m^{-2}$ and C_0 is set to 1.2 $mmol\ N.m^{-3}$. We can distinguish 5 regions. The first region corresponds to small values of μ_1 and μ_2 for which phytoplankton growth is too slow for them to subsist (fixed point n°1 in Table 2 for which eigenvalues λ_1 and λ_2 remain negative). When μ_1 or μ_2 are increased, fixed point n°1 loses its stability giving rise to fixed point n°2 or n°3 respectively (see Table 2). Further, if we keep increasing μ_1 or μ_2, fixed point n°4 or n°5 appears. For low C_0 value chosen on Fig. 7 neither μ_1 nor μ_2 values are able to give rise to a Hopf bifurcation. For higher C_0 values, this is observed (not shown).

In conclusion, μ_1 and μ_2 are likely to make the system undergo bifurcations between fixed points (transcritical bifurcation) and even between a fixed point

and a limit cycle (Hopf bifurcation, not shown). But their influence is all the same quite limited. Indeed, for $C_0 < \frac{m_p+\tau}{\tau}\frac{\varepsilon K}{g\beta-\varepsilon}$, growth rates just determine the transition between fixed points N^* and $N^*P_i^*$. Elsewhere in parameter space, given their domain of variation, μ_1 and μ_2 do not influence much the stable equilibria except close to transition lines of (I, C_0) bifurcation diagram. As expected μ_1 and μ_2 essentially play a role in the competition between the two phytoplankton species. If we refer to the (I, C_0) bifurcation diagram (Fig. 3), values of μ_1 and μ_2 act mainly on bifurcation curves which characterize a shift in the phytoplankton composition ($N^*P_1^* \leftrightarrow N^*P_2^*$ and $N^*P_1^*Z^* \leftrightarrow N^*P_2^*Z^*$). If μ_1 is increased, these curves move to the left on Fig. 3 in the (I, C_0)space, and conversely if μ_2 is increased.

3.3.3 Sensitivity to gross growth efficiency and ingestion rate (β and g)

The gross growth efficiency β for P_1 and P_2, and the maximum ingestion rate g appear in the grazing term and define its intensity. The bifurcation diagram as a function of these two parameters is presented on Fig. 8. The bifurcation curves have a hyperbolic signature, which suggests that the product $g\beta$ plays an essential role in bifurcation parameter. This is the case for $\lambda_5 = g\beta\frac{P_1^*}{K_Z+P_1^*} - \varepsilon$ (see Appendix A) whose zero curve is drawn on Fig. 8 (bifurcation $N^*P_1^* \leftrightarrow N^*P_1^*Z^*$). The product $g\beta$ has a quite important influence on the type of equilibrium solution (fixed point or limit cycle) reached by the system. If it is small, grazing is too weak so that zooplankton subsists. On the contrary, if it is important the system loses its stability and oscillations between variables occur. The global effect of βg on the general bifurcation diagram of Fig. 3 is as follows: an increase of βg induces a downward translation of bifurcation curves $N^*P_1^* \leftrightarrow N^*P_1^*Z^*$, $N^*P_2^* \leftrightarrow N^*P_2^*Z^*$

and $N^*P_1^*Z^* \leftrightarrow N^*P_2^*Z^*$, and also of the Hopf bifurcation curves. The parameters g and β have therefore mainly an influence on the temporal behaviour of the system at equilibrium. Like the re-mineralisation parameter, they can influence phytoplankton competition mainly for medium light values (corresponding to neighborhood of the bifurcation curve $N^*P_1^*Z^* \leftrightarrow N^*P_2^*Z^*$).

4 The ecosystem model behaviour in 1D diffusive dynamics

Knowing the intrinsic ecosystem model dynamics, its associated time scales and its sensitivity to parameters, we can now investigate the combined effect of diffusion and sedimentation processes on ecosystem structuring and more precisely on phytoplankton competition. For this purpose, we take exactly the same ecosystem model with the default parameter set presented in Table 1 and embed it into a simple physical model in which we define a profile of light, a profile of vertical diffusivity (Edwards et al., 2000) and a sedimentation speed on detritus. The important thing to notice is that light profile, diffusivity profile and sedimentation are constant in time. The purpose is to study the behaviour of the 1D model at equilibrium and to free ourselves of all temporal forcing. If sedimentation and diffusion are turned off, we have at each depth a OD ecosystem model running independently and following the behaviour described on Fig. 3 (called hereafter 'OD spatialized model'). If they are turned on, we have a 1D model with a vertical coupling of the different 0D simulations by physical dynamics.

The diffusivity coefficient K_v is vertically homogeneous in a surface layer (from 10^{-5} up to 10^{-1} $m^2.s^{-1}$) representing an idealized mixed layer of depth varying between 50 to 200 m. It is equal to a classical background value below the

mixed layer ($K_v = 10^{-5}\ m^2.s^{-1}$).

We chose to study the combined effect of diffusion and sedimentation and not the two processes separately to have a more realistic vertical water column. Without diffusion, the subsistence of an ecosystem at equilibrium is not possible, because all the organic matter would be gradually drained out from the euphotic layer. Furthermore, Hodges and Rudnick (2004) showed that the subsurface chlorophyll maximum is conditioned by the sedimentation rate on a biological compartment. Without sedimentation, organic matter gathers at surface. We chose a default sedimentation speed of 1 $m.day^{-1}$ so that 90 % of the organic matter is remineralised between 0 and 100 m in average. This is consistent with export ratio found at the base of the euphotic zone in various regions of the ocean (Schlitzer, 2000).

The light profiles used here are exponentially decreasing, $I = I_0 exp(\lambda z)$. I_0 is the surface irradiance. λ is the extinction coefficient and is set to 0.04 m^{-1}. The euphotic depth is defined as the depth where light is 1% of the surface irradiance. Here, we have a euphotic layer of 115 m depth. In this 1D configuration, the two phytoplankton species move in the light and total nitrogen gradients. All the simulations we discuss here are run until equilibrium.

In this study, we mainly vary the mixed layer depth, the diffusivity coefficient K_v and also the light profile, because in 0D light is essential to determine which phytoplankton species will survive. An idealized initial profile of nutrients based on tanh function is used. It is calibrated such as the nitracline depth is the same as the mixed layer depth. Initially nutrient are scarce in the mixed layer and abundant below. We first present the results for a winter case with a 200 m mixed layer and a surface irradiance of 111 $W.m^{-2}$ corresponding to midlatitudes (Campbell and Aarup, 1989). On Fig. 9, the verti-

cal ecosystem structuring is presented at equilibrium for two configurations with a mixed layer depth of 200 m and a diffusivity coefficient of respectively 10^{-3} $m^2.s^{-1}$ (Fig. 9a) and 10^{-2} $m^2.s^{-1}$ (Fig. 9b). On Fig. 9a, the two phytoplankton species coexist in the whole mixed layer whereas on Fig. 9b, there is a competitive exclusion of P_2. The first conclusion is that the combined diffusion and sedimentation processes can allow the coexistence of the two phytoplankton species at equilibrium which was absolutely impossible in 0D. Secondly, the result of the competition is very dependent on the diffusivity value resulting in competitive exclusion or coexistence of phytoplanktons.

To understand the mechanisms that lead to these different outcomes, Fig. 9c,d present the profiles that would be obtained without diffusion and sedimentation in the two cases ('OD spatialized model'). We take care to have the same C_0 profile as the one reached at the end of the previous 1D simulations. In practice, to obtain Fig. 9c,d, we run a new simulation from the C_0 profile of each balanced 1D simulation but this time, by cutting diffusion and sedimentation. Therefore, at each depth, the system reaches an equilibrium predicted by 0D analytical study. In the two cases, the '0D spatialized' simulations give the same kind of results i.e. the subsistence of P_1 in surface layers and P_2 below. The two phytoplankton species are maintained by zooplankton to a fixed concentration as described in the analytical study. To compare 0D predictions for light and amount of nutrients found along the water column and the 1D results, the corresponding (I, C_0) couples at each depth are reported on the bifurcation diagram established in the 0D analytical study (Fig. 9e,f). In 0D spatialized configuration, there is segregation of the two phytoplankton species with each profile of total nitrogen. But when the diffusion and sedimentation are turned on, we have totally different vertical ecosystem structuring: the weak K_v (Fig. 9a) induces the coexistence of the two phytoplankton species

whereas the strong K_v (Fig. 9b) induces the competitive exclusion of P_2. To analyse the mechanisms that lead to these results, we study the fluxes of biological variables as a function of time (not shown). The fluxes are integrated over a surface layer corresponding to the layer of P_1 dominance in 0D spatialized simulation, and over a subsurface layer where P_2 dominates in 0D.

They reveal that strong K_v induces quick nutrient injections into the mixed layer but P_2 growth is too slow to consume enough of them. Therefore these nutrients benefit P_1 which grows rapidly near the surface; P_1 growth is followed by that of Z. P_1 and Z propagate then downwards via diffusion; they enter the layer suitable for P_2 and weaken it. Furthermore, since P_1 uses all the nutrients in surface layer, the gradient in nutrients in the mixed layer is maintained and nutrients keep being diffused to the surface layer. This has again a negative feedback on P_2 which is more nutrient-limited and a positive one on P_1 which keeps developing and spreading downwards.

For weak K_v, on the contrary, P_2 is sufficiently rapid to consume a great part of the nutrients injected into the mixed layer. This limits the growth of P_1 and allows the coexistence of the two phytoplankton species in the whole mixed layer with a dominance of each of them in its prefered layer. Moreover, the integrated fluxes at equilibrium reveal that growth rate of P_2 (respectively P_1) is less than its loss rate in surface layer (respectively in subsurface layer). Indeed, the diffusive flux maintains P_2 in surface layer (respectively P_1 in subsurface layer). Thus, mixing allows a non-zero concentration of P_2 in the surface layer (respectively P_1 in the subsurface layer) where these phytoplanktons can not sustain their own population. In other words, there is a 'source' population which spreads phytoplankton in a hostile habitat. We have therefore coexistence between the two species despite mixing, that is to say even if mixing tends to create an isotropic environment without ecological niches that shel-

ter the weak species. And the magnitude of mixing makes the system shift between coexistence (intermediate mixing) or exclusion (strong mixing).

To complement these results retaining a winter mixed layer of 200 m depth, the surface irradiance is diminished to 50 $W.m^{-2}$ and then to 13 $W.m^{-2}$ which corresponds respectively to latitudes between 40 and 50°and polar latitudes (Campbell and Aarup, 1989). With these light profiles, P_2 is favoured over a thicker layer if we refer to 0D bifurcation diagram (see Fig. 3). For a surface irradiance of 50 $W.m^{-2}$, the results are the same as those previously shown. For a surface irradiance of 13 $W.m^{-2}$ (polar case), P_2 does exclude P_1 competitively when the diffusivity coefficient is set to 10^{-2} $m^2.s^{-1}$. It is what is expected from the 0D study.

After having shown the importance of the mixing magnitude in a winter case, we take a shallower mixed layer (30-50 m) associated to a summer light profile (surface irradiance of 230 $W.m^{-2}$). In this case, there is a vertical segregation (not shown): P_1 in the mixed layer and P_2 in the subsurface maximum. It is interesting to see that the mixed layer plays the role of an ecological niche for P_1. Each phytoplankton is sheltered from the other and can develop itself in its part of the water column.

Last, we checked that we obtained the same results as Edwards et al. (2000) who noticed a vanishing of oscillations when the ecosystem model was spatialized vertically. Mixing and sedimentation actually couple biological dynamics along vertical dimension. In our model, this has indeed a stabilizing effect on water column and limit cycles, predicted by 0D dynamics, become fixed points in 1D configuration.

To conclude on this 1D study, combined diffusion and sedimentation can al-

low coexistence of two species of phytoplankton at equilibrium even if there is always competitive exclusion in 0D. Furthermore, the value of the diffusivity coefficient is essential. Indeed, there is a threshold value for which the coupled system shifts from coexistence in the whole mixed layer to a competitive exclusion of P_2.

5 Discussion

The dynamics of an NPPZD ecosystem model was examined in the parameter space. The ecosystem structure, the type of equilibrium reached by the system (fixed point or limit cycle) and the value of each ecosystem variable at each fixed point has been obtained for each parameter set. This allowed us to deduce the parameter sensitivity and to conclude on the role of each parameter in ecosystem dynamics. Light intensity and total amount of nitrogen matter turn out to be the more important parameters. Because of their domain of variation, they allow a large variety of ecosystem structures and a large range of equilibrium values for each variable. Once a detailed knowledge of the 0D ecosystem dynamics was obtained, the model was embedded in a vertical environment. It allowed us to study the combined effect of diffusive physics and sedimentation of detritus. Diffusion and sedimentation turned out to have an important role in the ecosystem structure along the water column. They change the phytoplankton distribution and especially allow the coexistence of the two phytoplankton species at a same depth in the water column. 1D dynamics has also a stabilizing effect on the intrinsic oscillations displayed by a vertically-distributed ecosystem model.

We showed that the diffusivity coefficient K_v in the mixed layer determines

the outcome of the competition between the two phytoplankton species. More precisely, there is a threshold value beyond which one of the two species is competitively excluded. This competition result can be described by the classical diversity index of Shannon-Weaver H' as well. It is defined by $H' = -\sum_{i=1}^{2} \frac{P_i}{P_1+P_2} \log_2 \frac{P_i}{P_1+P_2}$. It varies between 0 and 1. This index is generally used with many species of phytoplankton. In our case, it is averaged in the mixed layer and it gives a quantification of coexistence (close to $H' = 1$) and exclusion or vertical segregation ($H' = 0$) and thus a new highlight of the results. The Shannon-Weaver index, averaged within the mixed layer, is plotted on Fig. 10a as a function of diffusivity. It shows an increase of H' with K_v between 10^{-5} to 2.10^{-3} $m^2.s^{-1}$ and a sharp decrease towards zero as soon as K_v exceeds a threshold value of 2.10^{-3} $m^2.s^{-1}$. This indicates a bifurcation of the 1D system between a fixed point with coexistence of the two phytoplankton species and a fixed point with competitive exclusion. Moreover, the maximum of H' is almost correlated with the maximum of total biomass (P_1+P_2+Z+D) in the system (Fig. 10b). It is slightly shifted from 1.10^{-3} $m^2.s^{-1}$. These model results are in line with enclosure experiments of Flöder and Sommer (1999) who showed that species diversity index H' reaches a maximum at intermediate level of disturbance (mixing).

Our '0D spatialized model' (Fig. 9c,d) shows that the two phytoplankton species are vertically segregated. Both of them survive at different levels because of the heterogeneity of the environmental conditions (I and C_0 vary along depth). Introducing vertical diffusion tends to mix this vertical distribution of phytoplankton and thus it is reasonable to expect a coexistence of the two phytoplankton species at a same depth. In the winter case, when the mixed layer is deeper than the euphotic layer, the two phytoplankton species have to face each other, with two solutions: either they coexist or one dies.

We showed that the outcome crucially depends on the value of diffusivity. If mixing is sufficiently weak (below a threshold value) phytoplankton almost does not feel the vertical gradients in 'physical parameters' (namely I and C_0). Each phytoplankton species develops in its preferential part of the mixed layer and then slowly diffuses in the whole mixed layer. Thus the two phytoplankton species coexist. If, on the contrary, mixing is sufficiently intense, light and total nitrogen received by the two phytoplankton species have an amplitude that is about the average of I and C_0 in the mixed layer. In this case, physical and biological dynamics decouple and the results become identical to those of the 0D model (competitive exclusion).

In this study we considered a model with an intermediate level of complexity to address the question of phytoplankton competition: two phytoplankton species competing for one nutrient and light. Without external forcing (0D model), light is a fixed parameter. There are more phytoplankton species than limiting resources. As a consequence, we observe a competitive exclusion of one phytoplankton whatever the parameters in accordance with the competitive exclusion principle (Hardin, 1960). In the 1D model things are less simple: the fixed vertical gradient of light combined with the physical forcing induced by vertical mixing may be thought as an "active" limiting factor. Therefore we should expect a possible coexistence of the two phytoplankton species on the two limiting factors. This is why we have also tested a three-phytoplankton species model competing for the same two resources (light and nutrient) to see if vertical mixing is always able to make these three phytoplankton species coexist. The results are shown on Fig. 11. The ecosystem model used here is very similar to the one previously studied but now with three phytoplankton species: one better adapted to surface conditions, a second better adapted to intermediate depths, and the third better adapted to even deeper depths. Pa-

rameters of the three phytoplankton are indicated in Table 3. As expected, the 0D model predicts a competitive exclusion of two phytoplankton species at each point of the parameter space. But Fig. 11 reveals a coexistence of the three phytoplankton species together over the mixed layer which confirms our preceding results : the effect of vertical mixing is able to maintain a greater number of phytoplankton species than the number of limiting resources. Therefore, this one-dimensional process is another potential answer to the 'paradox of plankton' in the sense that it is able to prevent the competitive exclusion of one or more phytoplankton species at equilibrium.

This two or three species coexistence at equilibrium can be explained by the coupling between mixing and biological dynamics. Let us describe the different time scales inherent in the system and then discuss the possible influence of turbulent vertical injections of nutrients in the mixed layer. The ecosystem time scales determined in the analytical study (Fig. 5) were 1-5 days in surface layer, and 10-20 days in subsurface. The ecosystem could also undergo self-sustained oscillations with periods of about 50 days. Concerning one-dimensional dynamics, a diffusivity coefficient of 10^{-4} to 10^{-2} $m^2.s^{-1}$ corresponds to time scales of around 100 to 1 days respectively if we consider a vertical length scale of 25 m corresponding to the scale of the nutrient gradient. These similar time scales show that, in the mixed layer, diffusion may interact with ecosystem dynamics and couple the ecosystems at different depths. This explains the strong sensitivity of the ecosystem structuring to the diffusivity value revealed by 1D simulations.

Lastly, if we consider a three-dimensional environment, time scales corresponding to turbulent vertical injections can be estimated. To schematize, we classify oceanic motions in three scales: large scale, mesoscale and submesoscale. The

first one corresponds for instance to wind-induced gyres with horizontal scales of a few thousand kilometers and with vertical time scales of the order of 100-1000 days (around 300 days according to Flierl and McGillicuddy, 2002). The second one corresponds to phenomena like eddies or meanders, characterized by length scale of about 100 km and time scales of 10-100 days (Klein and Lapeyre, 2009). The last class results from the interaction between mesoscale structures which forms filaments characterized by strong gradients on scales of 10 km. The time scale of nutrient injections in these filaments is about 1 day (Klein and Lapeyre, 2009). The comparison of these time scales with biological ones indicates how efficient the coupling between physical and biological dynamics can be.

Ecosystem time scales were diagnosed in the analytical study (Fig. 5). At large scale and in surface layers, ecosystem dynamics is therefore expected to be much faster than ocean dynamics so the ecosystem feels the evolution of physical environment as a change in initial conditions. Immediately, it reacts to the perturbation and reaches a new fixed point. Thus, the 0D ecosystem model predictions concerning phytoplankton competition should be similar to in situ data in a weakly turbulent domain. Our model predicts a dominance of the small species (picophytoplankton P_1), which is in accordance with data collected during several surveys. Indeed, Claustre et al. (1994) reported a dominance of cyanobacteria and flagellates (nano- and pico- phytoplankton) in surface layers in the areas adjacent to the front between Mediterranean and Atlantic waters whereas the frontal zone was diatom-dominated. Dandonneau et al. (2006) also showed a clear dominance of picophytoplankton (75%) at sea surface of South Pacific subtropical gyre (highly oligotrophic region). The results of Vidussi et al. (2001) also confirm this clear dominance and stability of small phytoplankton species in surface waters at large scale. They show the

predominance of pico- and nano- phytoplankton in oligotrophic areas of the Levantine basin (eastern Mediterranean).

Deeper in the ocean, conclusions seem to be less simple. Physics and biology evolve approximately at the same rate. Our ecosystem model, at equilibrium, predicts either a fixed point with an associated time scale of 10-20 days or self-sustained oscillations with a 50-day period. But ocean dynamics might disguise these potential oscillations (Koszalka et al., 2007). It might account for the very few observations of fluctuations of the deep chlorophyll maximum. Only Huisman et al. (2006) reported such sustained oscillations in oligotrophic waters of subtropical Pacific Ocean and ascribed it to intrinsic ecosystem dynamics (and not to seasonal forcing).

At meso- and submeso- scale, data are still too scarce and scattered for us to be able to draw a conclusion. According to a few studies (Fryxell et al., 1985; Vidussi et al., 2001; Jeffrey and Hallegraeff, 1980) it seems that at sea surface, at eddy edge, there is a shift in size of the phytoplankton community structure towards small species (pico- and nano-phytoplankton). But these observations are difficult to relate to biological and physical time scales.

At eddy centre, there is no rule either. Phytoplankton dominance depends on the class of motion (cyclone, anticyclone, mode-water eddy) and on the eddy age (Claustre et al., 1994; Fryxell et al., 1985; Vidussi et al., 2001; Sweeney et al., 2003; Vaillancourt et al., 2003; Jeffrey and Hallegraeff, 1980). This variety of ecosystem size distribution in eddy centre seems to support the hypothesis that physics and biology are indivisible at this scale. Ecosystems are presumably never at equilibrium. At meso- and submeso-scale, high biodiversity observed may thus be explained by non-equilibrium conditions imposed by physical forcing. Ocean submeso- and mesoscale structures should play a role

of shelter for less-competitive species and thus allow them to survive (Bracco et al., 2000; Pasquero et al., 2004).

The purpose of this study was to focus on the dynamics of an NPPZD ecosystem and on its behaviour when submitted to mixing, and particularly in terms of phytoplankton competition. The spatially extended and coupled system exhibits a wider range of ecosystem structures, allowing for instance coexistence between the two phytoplankton species over the first 200 meters of the water column. This provides an additional solution to the 'paradox of the plankton', complementing the overview drawn up by Roy and Chattopadhyay (2007). The examination of physical and biological time scales allowed us to conclude on the likely coupling between ecosystem and ocean dynamics in three dimensions, except in weakly-turbulent ocean surface layers. Further work has to be done in new numerical process studies using simplified three-dimensional ocean dynamics models, including 3D advection (at mesoscale and submesoscale) and interactions with mixed layer dynamics for instance. These new process studies should complement our conclusions issued from the timescale analysis, in particular concerning the influence of fine scale dynamical structures on phytoplankton competition within an ecosystem.

Acknowledgements

This work was funded by the INSU-CNRS CYBER-LEFE programme through the TWISTED action, and the french research ministry.

List of Tables

List of Figures

Parameter	Value	Unit	Description
Phytoplanktons			
μ_1	1.9	day^{-1}	Maximal P_1 growth rate
μ_2	1.5	day^{-1}	Maximal P_2 growth rate
K_{N1}	0.15	$mmol\ N.m^{-3}$	Half saturation constant of P_1 for nutrient uptake
K_{N2}	0.6	$mmol\ N.m^{-3}$	Half saturation constant of P_2 for nutrient uptake
K_{I1}	30	$W.m^{-2}$	P_1 affinity for light
K_{I2}	5	$W.m^{-2}$	P_2 affinity for light
m_p	0.045	day^{-1}	Phytoplankton mortality rate
Zooplankton			
g	1.5	day^{-1}	Maximum ingestion rate
Kz	1.4	$mmol\ N.m^{-3}$	Half saturation constant for ingestion
β	0.2		Gross Growth Efficiency for P_1 and P_2
ε	0.06	day^{-1}	Mortality rate
Detritus			
τ	0.1	day^{-1}	Specific remineralisation rate

Table 1
Ecosystem model parameters

n°	Ecosystem structure	Temporal behaviour
1	N	Fixed Point
2	NP_1	Fixed Point
3	NP_2	Fixed Point
4	NP_1Z	Fixed Point and Limit Cycle
5	NP_2Z	Fixed Point and Limit Cycle
6	NP_1P_2	-
7	NP_1P_2Z	-

Table 2
The different nonlinear equilibria of the ecosystem model

Parameter	Value	Unit	Description
μ_1	1.7	day^{-1}	Maximal P_1 growth rate
μ_2	1.7	day^{-1}	Maximal P_2 growth rate
μ_3	1.3	day^{-1}	Maximal P_3 growth rate
K_{N1}	0.15	$mmol\ N.m^{-3}$	Half saturation constant of P_1 for nutrient uptake
K_{N2}	0.4	$mmol\ N.m^{-3}$	Half saturation constant of P_2 for nutrient uptake
K_{N3}	1	$mmol\ N.m^{-3}$	Half saturation constant of P_3 for nutrient uptake
K_{I1}	25	$W.m^{-2}$	P_1 affinity for light
K_{I2}	5	$W.m^{-2}$	P_2 affinity for light
K_{I3}	1	$W.m^{-2}$	P_3 affinity for light

Table 3
3 phytoplankton ecosystem model: Parameters of the three phytoplankton species P_1, P_2, P_3. All the other parameters are the same as in Table 1

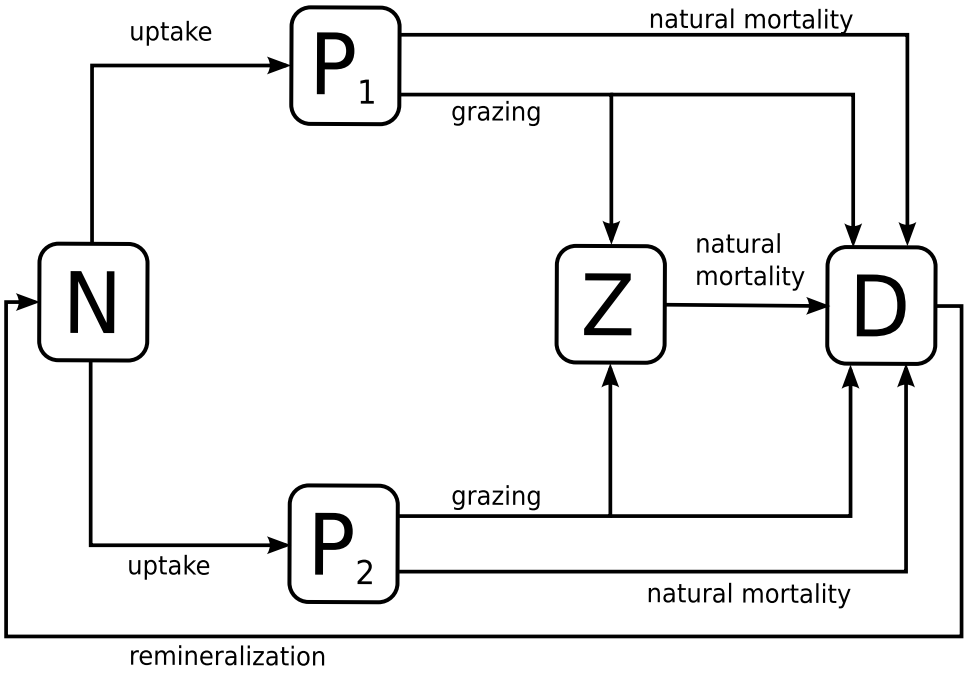

Fig. 1. Structure of the five-component ecosystem model: nitrate (N), small phytoplankton (P_1), large phytoplankton (P_2), zooplankton (Z) and detritus (D).

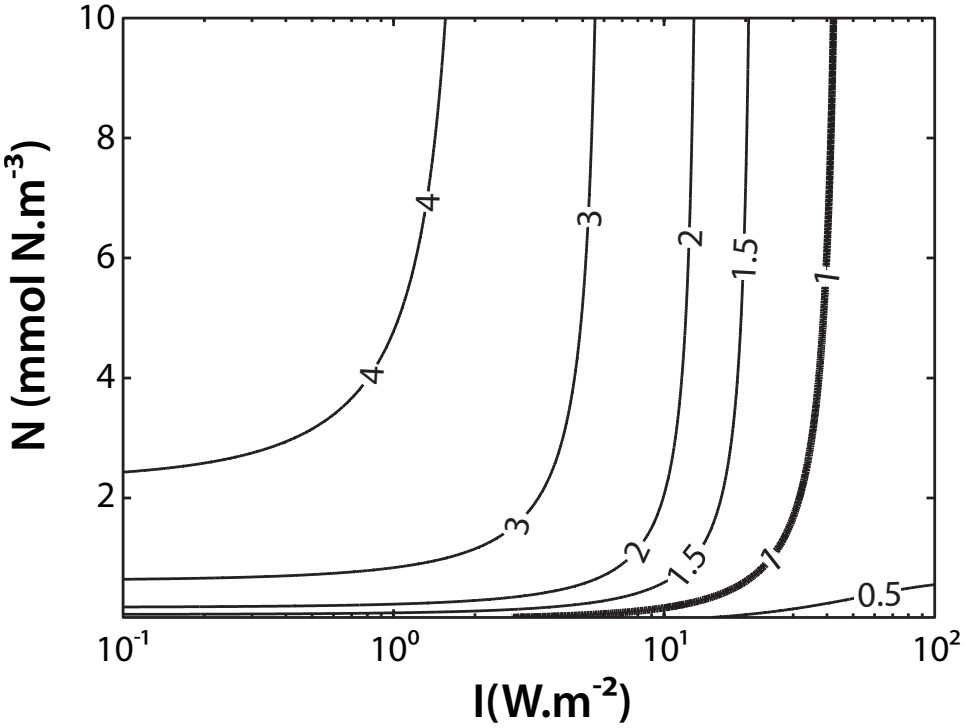

Fig. 2. Ratio between P_2 and P_1 effective growth rates as a function of light (I) and concentration of nutrients (N).

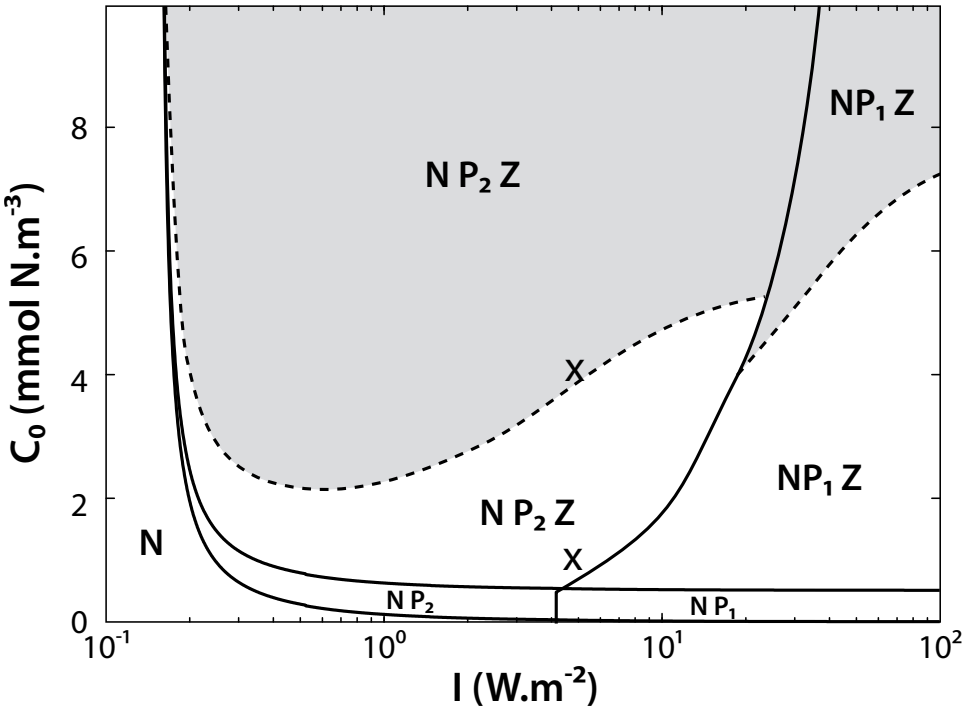

Fig. 3. Bifurcation diagram as a function of light I ($W.m^{-2}$) and total amount of nitrogen matter C_0 ($mmol\ N.m^{-3}$) for the default biological parameters given in Table 1. Grey areas indicate limit cycle equilibrium (other equilibria are fixed points). The two crosses indicate the location of (I,C_0) couples used to explore the sensitivity of the model to other parameters.

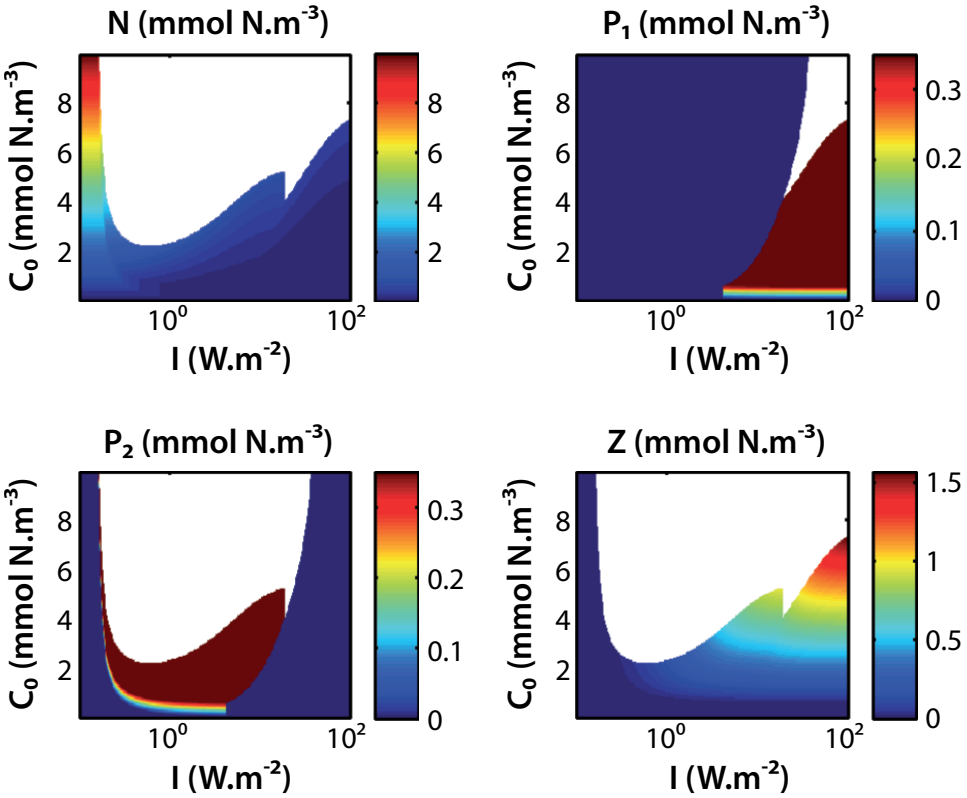

Fig. 4. Equilibrium values of N, P_1, P_2 and Z as a function of light I and total amount of nitrogen matter C_0. Biological parameters are default parameters given in Table 1.

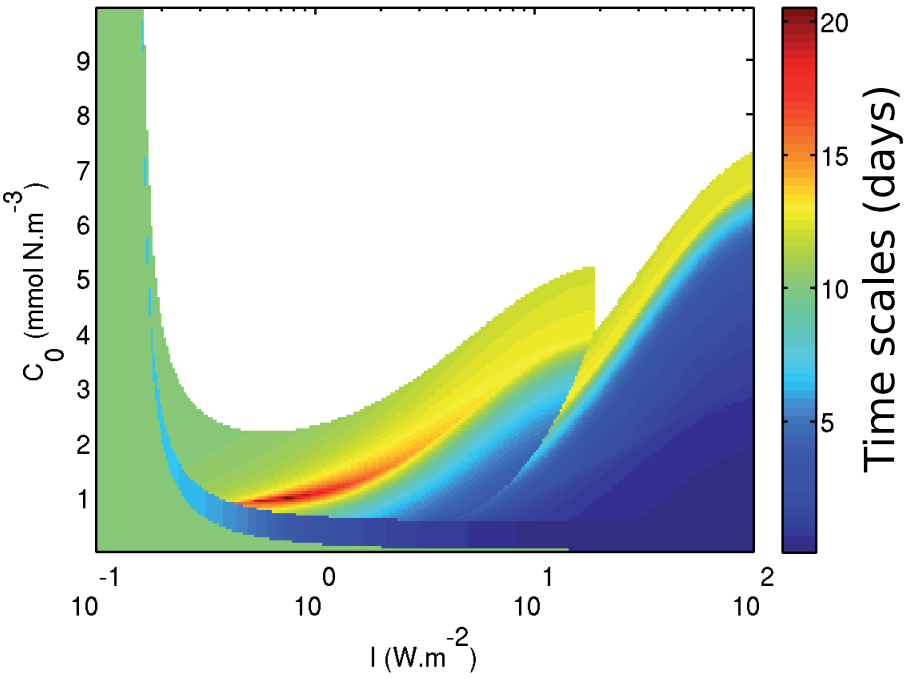

Fig. 5. Time scales (days) of the ecosystem model at fixed points as a function of light I $(W.m^{-2})$ and total amount of nitrogen C_0 $(mmol\ N.m^{-3})$.

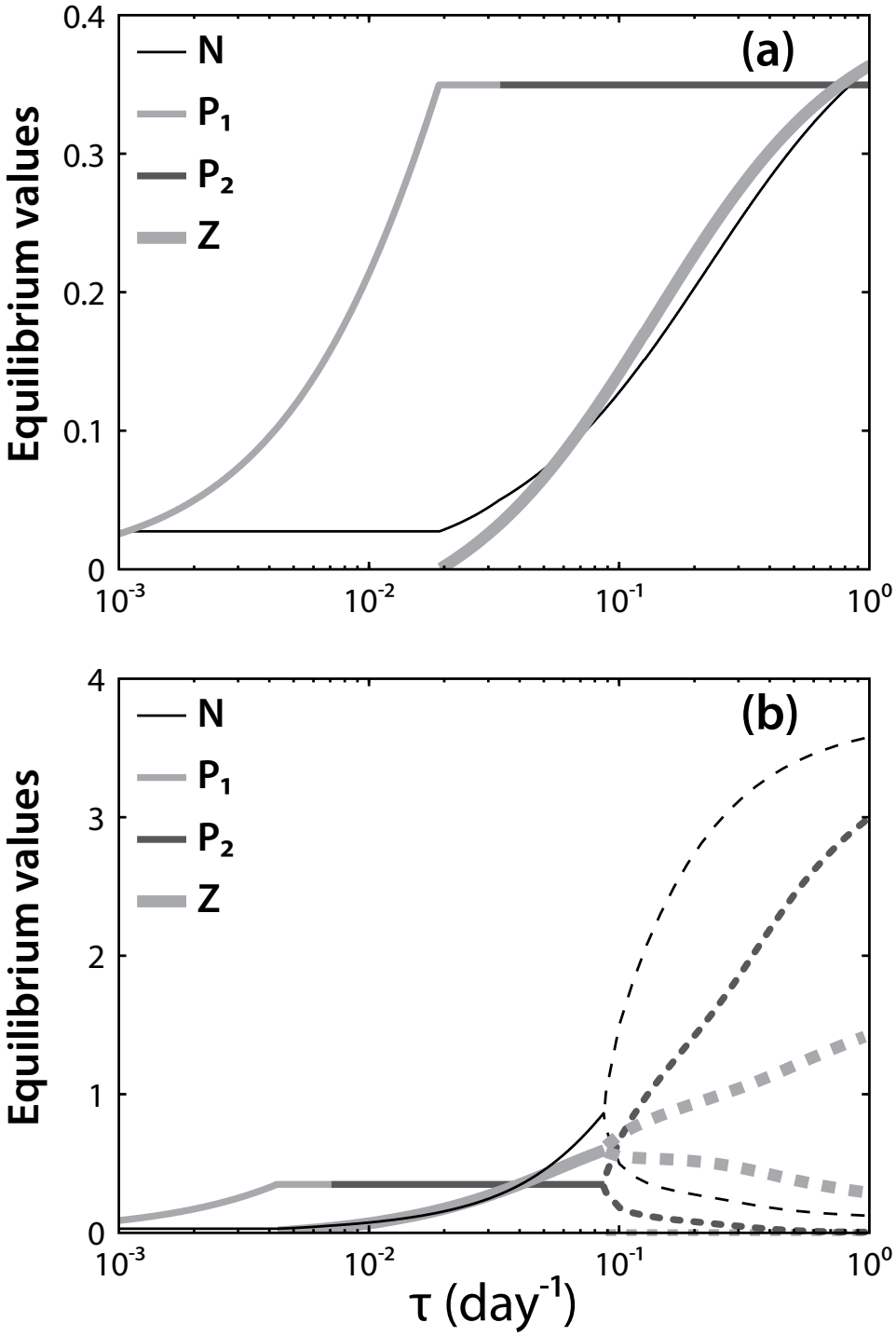

Fig. 6. Equilibrium values ($mmol\ N.m^{-3}$) of N, P_1, P_2 and Z as a function of re-mineralisation parameter τ; I set to 5 $W.m^{-2}$ and (a) C_0 set to 1.2 $mmol\ N.m^{-3}$, (b) C_0 set to 4 $mmol\ N.m^{-3}$. The fixed points are represented with solid lines, minimum and maximum values of limit cycles are represented with dashed lines. All the other biological parameters are default parameters given in Table 1.

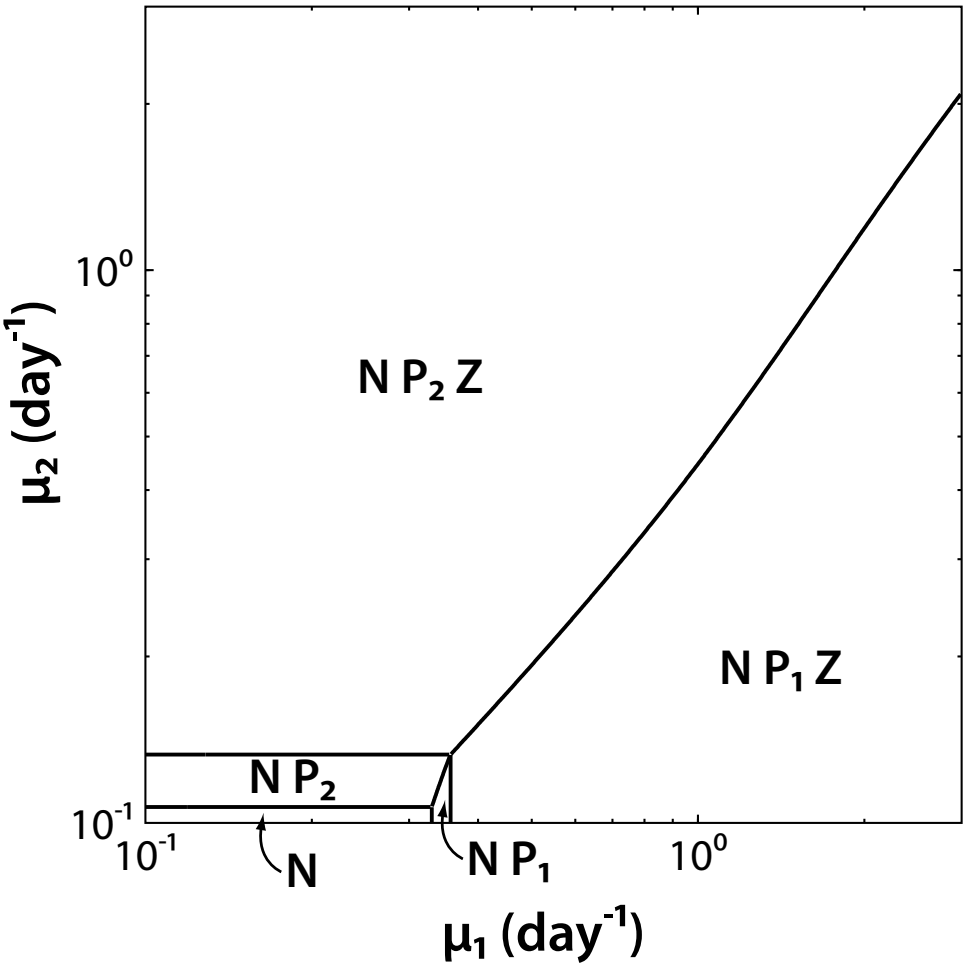

Fig. 7. Bifurcation diagram as a function of phytoplankton growth rates μ_1 and μ_2; I set to 5 $W.m^{-2}$, C_0 set to 1.2 $mmol\ N.m^{-3}$. All the other biological parameters are default parameters given in Table 1.

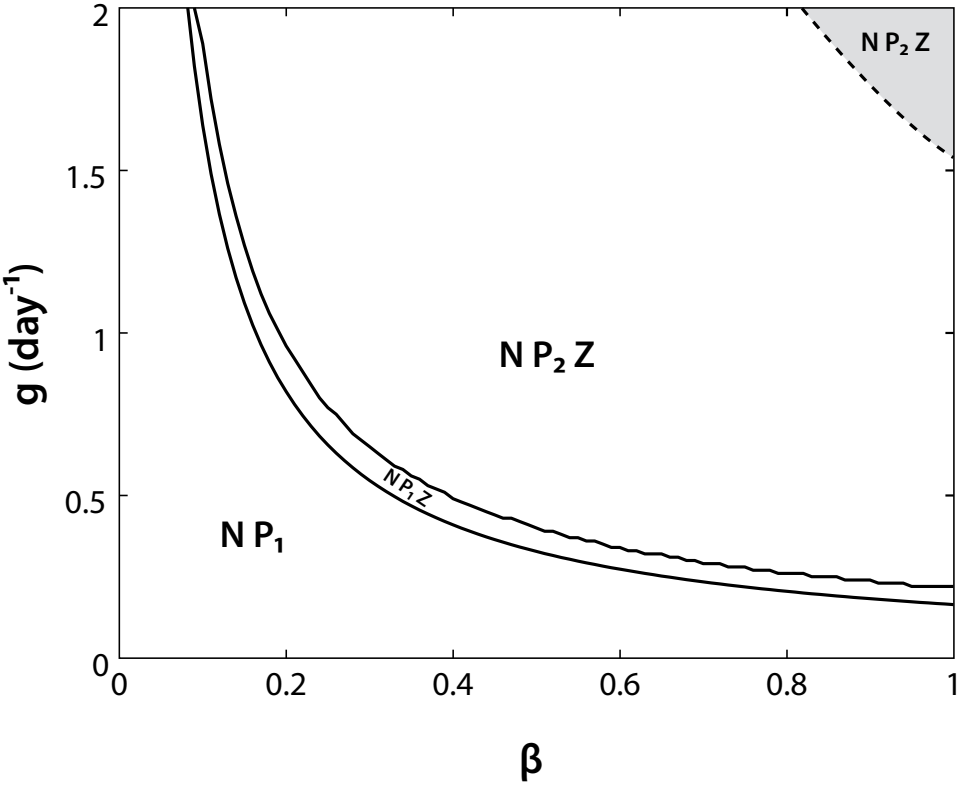

Fig. 8. Bifurcation diagram as function of zooplankton parameters: gross growth efficiency β and maximum ingestion rate g; I set to 5 $W.m^{-2}$, C_0 set to 1.2 $mmol\ N.m^{-3}$.Grey areas indicate limit cycle equilibrium (other equilibria are fixed points).

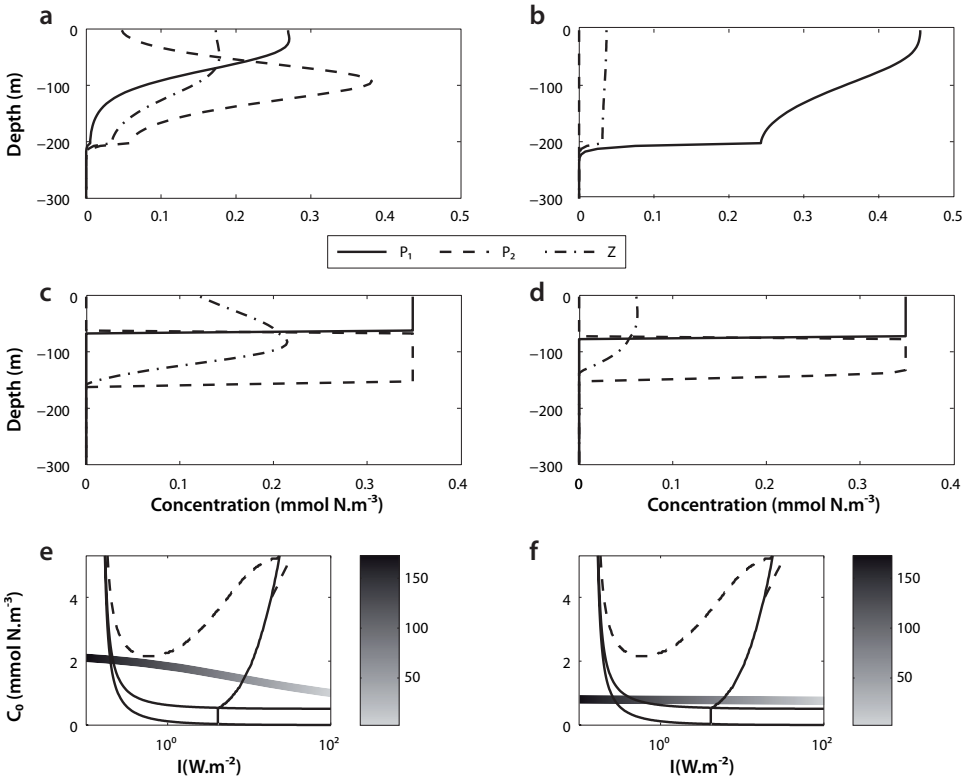

Fig. 9. Top panels: Ecosystem structuring in 1D simulations with a 200 m depth mixed layer. Profiles of P_1 (solid line), P_2 (dashed line) and Z (dashed-dotted line) at equilibrium with diffusivity coefficient in the mixed layer: (a) $K_v = 10^{-3}\ m^2.s^{-1}$, (b) $K_v = 10^{-2}\ m^2.s^{-1}$. Middle panels: Ecosystem structuring in 0D spatialized simulations. Profiles of P_1 (solid line), P_2 (dashed line) and Z (dashed-dotted line) at equilibrium: (c) C_0 profile same as (a), (d) No mixing and C_0 profile same as (b). Bottom panels: Bifurcation diagram with (I, C_0) couples at each depth: (e) C_0 profile same as (a), (f) C_0 profile same as (b)

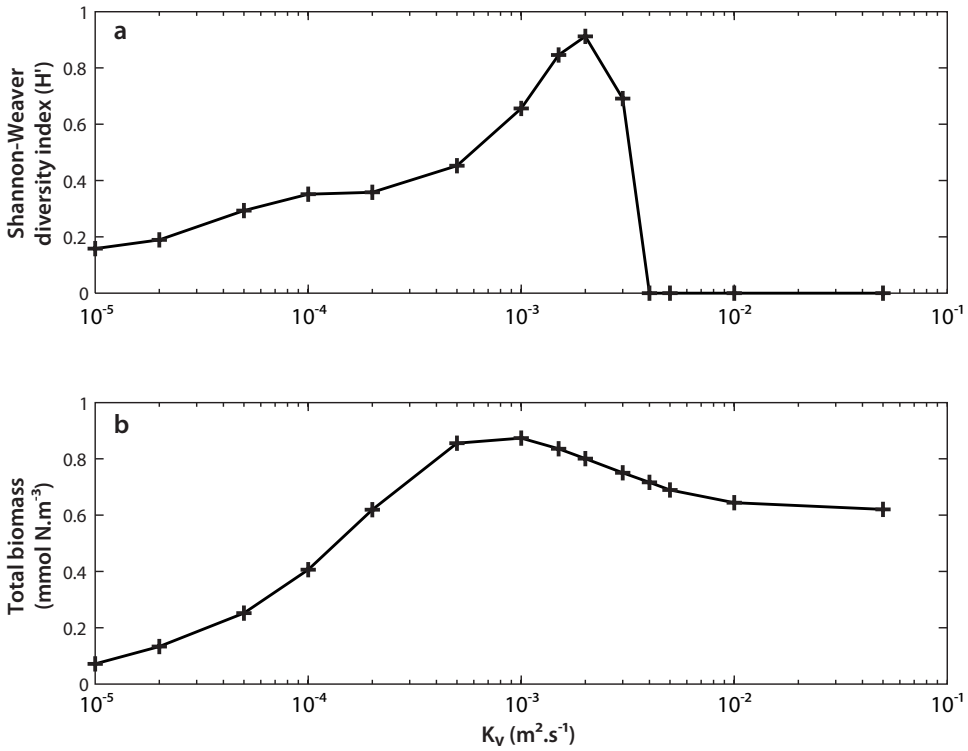

Fig. 10. (a) Vertical mean of Shannon-Weaver Diversity index H as a function of diffusivity coefficient K_v; Mixed layer depth of 200 m (b) Total biomass (P_1+P_2+Z+D in $mmol\ N.m^{-3}$) as a function of diffusivity coefficient K_v

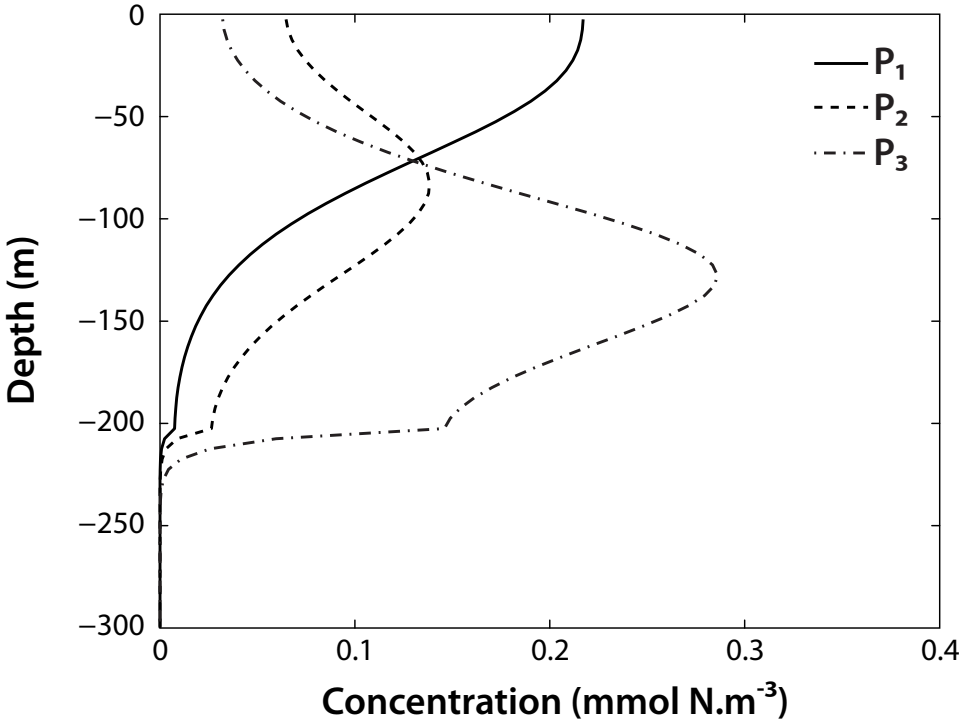

Fig. 11. 1D simulation with 3 phytoplankton species: Vertical profile of P_1, P_2 and P_3 at equilibrium with a 200 m depth mixed layer and $K_v = 10^{-3}\ m^2.s^{-1}$. P_1 (solid line) is better adapted to surface conditions, P_2 (dashed line) to intermediate depths and P_3 (dashed dotted line) to even deeper depths.

References

Agustí, S., Satta, M., Mura, M., Benavent, E., 1998. Dissolved esterase activity as a tracer of phytoplankton lysis: evidence of high phytoplankton lysis rates in the northwestern Mediterranean. Limnology and Oceanography, 1836–1849.

Anderson, T., 2005. Plankton functional type modelling: running before we can walk? Journal of Plankton Research 27, 1073–1081.

Banse, K., 1982. Cell volumes, maximal growth rates of unicellular algae and ciliates, and the role of ciliates in the marine pelagial. Limnol. Oceanogr 27 (105), 9–107.

Benincà, E., Huisman, J., Heerkloss, R., Johnk, K., Branco, P., Van Nes, E., Scheffer, M., Ellner, S., 2008. Chaos in a long-term experiment with a plankton community. Nature 451 (7180), 822–825.

Biddanda, B., Pomeroy, L., 1988. Microbial aggregation and degradation of phytoplankton-derived detritus in seawater. I. Microbial succession. Marine ecology progress series. Oldendorf 42 (1), 79–88.

Bracco, A., Provenzale, A., Scheuring, I., 2000. Mesoscale vortices and the paradox of the plankton. Proceedings of the Royal Society of London (B) 267, 1795–1800.

Busenberg, S., Kumar, S., Austin, P., Wake, G., 1990. The dynamics of a model of a plankton-nutrient interaction. Bulletin of Mathematical Biology 52 (5), 677–696.

Campbell, J., Aarup, T., 1989. Photosynthetically available radiation at high latitudes. Limnology and Oceanography, 1490–1499.

Claustre, H., Kerhervé, P., Marty, J.-C., Prieur, L., Videau, C., Hecq, J.-Y., 1994. Phytoplankton dynamics associated with a geostrophic front: Eco-

logical and biogeochemical implications. Journal of Marine Research 52, 711–742.

Dandonneau, Y., Montel, Y., Blanchot, J., Giraudeau, J., Neveux, J., 2006. Temporal variability in phytoplankton pigments, picoplankton and coccolithophores along a transect through the north atlantic and tropical southwestern pacific. Deep-Sea Research I 53, 689–712.

Denman, K., Pena, M., 1999. A coupled 1-D biological/physical model of the northeast subarctic Pacific Ocean with iron limitation. Deep-Sea Research Part II 46 (11-12), 2877–2908.

Edwards, A., Brindley, J., 1999. Zooplankton mortality and the dynamical behaviour of plankton population models. Bulletin of mathematical biology 61 (2), 303–339.

Edwards, A. M., 2001. Adding detritus to a nutrient-phytoplankton-zooplankton model: a dynamical-systems approach. Journal of Plankton Research 23, 389–413.

Edwards, C., Powell, T., Batchelder, H., 2000. The stability of an NPZ model subject to realistic levels of vertical mixing. Journal of Marine Research 58 (1), 37–60.

Fasham, M., Ducklow, H., McKelvie, S., 1990. A nitrogen-based model of plankton dynamics in the oceanic mixed layer. Journal of Marine Research 48 (3), 591–639.

Flierl, G., McGillicuddy, D., 2002. Mesoscale and submesoscale physical-biological interactions. The Sea 12, 113–185.

Flöder, S., Sommer, U., 1999. Diversity in planktonic communities: An experimental test of the intermediate disturbance hypothesis. Limnology and Oceanography 44 (4), 1114–1119.

Franks, P., Wroblewski, J., Flierl, G., 1986. Behavior of a simple plankton

model with food-level acclimation by herbivores. Marine Biology 91 (1), 121–129.

Fryxell, G., Gould, R., Balmori, E., Theriot, E., 1985. Gulf Stream warm core rings: phytoplankton in two fall rings of different ages. Journal of Phytoplankton Research 7, 339–364.

Hardin, G., 1960. The Competitive Exclusion Principle. Science 131 (3409), 1292–1297.

Harrison, W., Harris, L., Irwin, B., 1996. The kinetics of nitrogen utilization in the oceanic mixed layer: Nitrate and ammonium interactions at nanomolar concentrations. Limnology and Oceanography 41 (1), 16–32.

Hirst, A., Kiørboe, T., 2002. Mortality of marine planktonic copepods: global rates and patterns. Marine Ecology Progress Series 230, 195–209.

Hodges, B. A., Rudnick, D. L., 2004. Simple models of steady deep maxima in chlorophyll and biomass. Deep-Sea Research I 51, 999–1015.

Huisman, J., Pham Thi, N. N., Karl, D., Sommeijer, B., 2006. Reduced mixing generates oscillations and chaos in the oceanic deep chlorophyll maximum. Nature 439, 322–325.

Huisman, J., Weissing, F. J., 1999. Biodiversity of plankton by species oscillations and chaos. Nature 402, 407–410.

Hutchinson, G., 1961. The paradox of the plankton. The American Naturalist 95, 137–145.

Jeffrey, S., Hallegraeff, G., 1980. Studies of phytoplankton species and photosynthetic pigments in a warm core eddy of the east australian current. i. summer populations. Marine Ecology Progress Series 3, 285–294.

Kiørboe, T., 1997. Population regulation and role of mesozooplankton in shaping marine pelagic food webs. Hydrobiologia 363 (1), 13–27.

Klein, P., Lapeyre, G., 2009. The oceanic vertical pump induced by mesoscale

842 turbulence. Annual Review of Marine Science 1, 361–375.
843 Koszalka, I., Bracco, A., Pasquero, C., Provenzale, A., 2007. Plankton cycles
844 disguised by turbulent advection. Journal of Theoretical Biology.
845 Krivan, V., 1996. Optimal Foraging and Predator–Prey Dynamics. Theoretical
846 Population Biology 49 (3), 265–290.
847 Krivan, V., 1997. Dynamic Ideal Free Distribution: Effects of Optimal Patch
848 Choice on Predator-Prey Dynamics. American Naturalist 149 (1), 164–178.
849 Lima, I. D., Olson, D. B., Doney, S. C., 2002a. Biological response to frontal
850 dynamics and mesoscale variability in oligotrophic environments: Biological
851 production and community structure. Journal of Geophysical Research 107,
852 25–1.
853 Lima, I. D., Olson, D. B., Doney, S. C., 2002b. Intrinsic dynamics and stability
854 properties of size-structured pelagic ecosystem models. Journal of Plankton
855 Research 24, 533–556.
856 Lønborg, 2009. Bioavailability and bacterial degradation rates of dissolved
857 organic matter in a temperate coastal area during an annual cycle. Marine
858 chemistry In press, Corrected Proof ("").
859 Marbà, N., Duarte, C., Agustí, S., 2007. Allometric scaling of plant life history.
860 Proceedings of the National Academy of Sciences 104 (40), 15777.
861 Margalef, R., 1958. Temporal succession and spatial heterogeneity in phyto-
862 plankton. Perspectives in marine biology, 323–349.
863 Martin, A. P., Richards, K. J., Fasham, M. J., 2001. Phytoplankton production
864 and community structure in an unstable frontal region. Journal of Marine
865 Systems 28, 65–89.
866 McCauley, E., Murdoch, W., 1987. Cyclic and stable populations: plankton as
867 paradigm. American Naturalist, 97–121.
868 McGurk, M., 1986. Natural mortality of marine pelagic fish eggs and larvae:

role of spatial patchiness. Mar. Ecol. Prog. Ser. 34, 227–242.

Moloney, C., Field., J., 1989. General allometric equations for rates of nutrient uptake, ingestion, and respiration in plankton organisms. Limnol. Oceanogr 34 (7), 1290–1299.

Moloney, C., Field, J., 1991. The size-based dynamics of plankton food webs. I. A simulation model of carbon and nitrogen flows. Journal of Plankton Research 13 (5), 1003–1038.

Newell, R., Lucas, M., Linley, E., 1981. Rate of degradation and efficiency of conversion of phytoplankton debris by marine microorganisms. Mar. Ecol. Prog. Ser 6, 123–136.

Olson, D., Hood, R., 1994. Modelling pelagic biogeography. Progress in Oceanography 34 (2), 161–205.

Panagiotopoulos, C., Sempéré, R., Obernosterer, I., Striby, L., Goutx, M., Van Wambeke, F., Gautier, S., Lafont, R., 2002. Bacterial degradation of large particles in the southern Indian Ocean using in vitro incubation experiments. Organic Geochemistry 33 (8), 985–1000.

Pasquero, C., Bracco, A., Provenzale, A., 2004. Coherent vortices, lagrangian particles and the marine ecosystem. Shallow flows, 399–412.

Passarge, J., Huisman, J., 2002. Competition in well-mixed habitats: From competitive exclusion to competitive chaos. Ecological Studies 161, 7–42.

Riley, G., 1957. Phytoplankton of the north central sargasso sea, 1950-52. Limnology and Oceanography 2, 252–270.

Rivière, P., Pondaven, P., 2006. Phytoplankton size classes competitions at sub-mesoscale in a frontal oceanic region. Journal of Marine Systems 60, 345–364.

Roy, S., Chattopadhyay, J., 2007. Towards a resolution of the paradox of the plankton: A brief overview of the proposed mechanisms. Ecological Com-

plexity 4 (1-2), 26–33.

Schlitzer, R., 2000. Applying the adjoint method for biogeochemical modeling: export of particulate organic matter in the world ocean. GEOPHYSICAL MONOGRAPH-AMERICAN GEOPHYSICAL UNION 114, 107–124.

Steele, J., Henderson, E., 1992. The role of predation in plankton models. Journal of Plankton Research 14 (1), 157–172.

Straile, D., 1997. Gross growth efficiencies of protozoan and metazoan zooplankton and their dependence on food concentration, predator-prey weight ratio, and taxonomic group. Limnology and Oceanography 42 (6), 1375–1385.

Sweeney, E., McGillicuddy, D., Buesseler, K., 2003. Biogeochemical impacts due to mesoscale eddy activity in the sargasso sea as measured et the bermuda atlantic time-series study (bats). Deep-Sea Research II 50, 3017–3039.

Taguchi, S., 1976. Relationship between photosynthesis and cell size of marine diatoms. J. Phycol 12 (2), 185–189.

Vaillancourt, R., Marra, J., Seki, M., Parsons, M., Bidigare, R., 2003. Impact of a cyclonic eddy on phytoplankton community structure and photosynthetic competency in the subtropical north pacific ocean. Deep-Sea Research I 50, 829–847.

Vidussi, F., Claustre, H., Manca, B., Luchetta, A., Marty, J.-C., 2001. Phytoplankton pigment distribution in relation to upper thermocline circulation in the eastern mediterranean sea during winter. Journal of Geophysical Research 106, 939–956.

Wroblewski, J., O'Brien, J., 1976. A spatial model of phytoplankton patchiness. Marine Biology 35 (2), 161–175.

Appendix

A Calculation of the equilibria

It can be easily shown that for such an ecosystem, no trivial equilibrium can be attained if $N = 0$ or $N = P_1 = P_2 = 0$ (in other words phytoplankton needs nutrients to survive and zooplankton needs phytoplankton to survive). A fixed point (defined by $f(X, \nu) = 0$) becomes unstable if any eigenvalue of its Jacobian matrix has a real part which becomes positive as parameters vary. The condition for this change of sign can be translated into a relation between the parameters (here C_0 and I for instance). This relation defines a bifurcation curve between two equilibria. When this change of sign occurs for a single eigenvalue, the new equilibrium is a fixed point and the bifurcation is called transcritical. When it occurs for a pair of complex conjugate eigenvalues, the new attractor is a limit cycle reached via a Hopf bifurcation. When a fixed point is stable, the smallest inverse of the negative real part of its eigenvalues defines the e-folding time T. When the equilibrium is slightly perturbed, T is the time needed for this perturbation to decrease by a factor e in the return to equilibrium. State variables at a fixed point will be refered to with the symbol '*'.

Fixed point n°1: This is the trivial "no life" equilibrium ($N^* = C_0$, $P_1^* = P_2^* = Z^* = 0$) corresponding for instance to the deep ocean or the nutrient depleted surface layer. This fixed point is defined in the whole parameter space but becomes unstable as soon as any phytoplankton species is able to develop.

The eigenvalues of the Jacobian matrix at this fixed point are the following:

$$\lambda_1 = \alpha_1 \frac{C_0}{K_{N1} + C_0} - m_p$$

$$\lambda_2 = \alpha_2 \frac{C_0}{K_{N2} + C_0} - m_p$$

$$\lambda_3 = -\tau$$

$$\lambda_4 = -\varepsilon$$

Among them, the first two (λ_1 and λ_2) are the bifurcation parameters (they are real and can change sign) unlike the last two (λ_3 and λ_4) which are always real negative because of the ecosystem parameter positivity. λ_1 is associated with a bifurcation towards fixed point $N^* P_1^*$ whereas λ_2 is associated with a bifurcation towards fixed point $N^* P_2^*$. Thus these two bifurcation parameters are fundamental to understand the competition between phytoplankton species : as soon as λ_1 (respectively λ_2) becomes positive, P_1 (respectively P_2) emerges and excludes P_2 (respectively P_1). As expected, parameters $\mu_i, K_{N\,i}$, and $K_{I\,i}$, which define the phytoplankton competitiveness for light and nutrients, constrain the emergence of one or the other phytoplankton. The fixed point destabilizes all the faster as the values of parameters C_0, I, μ_1 and μ_2 are higher or $K_{N1}, K_{N2}, K_{I1}, K_{I2}$ and m_p are lower.

Here, depending on the ecosystem parameter values, either $T = 1/\tau$ or $T = 1/\varepsilon$ or $T > 1/m_p$. Given the permitted values (discussed before), we can say that $T = 1/\tau$ over a large part of the parameter space. With the default parameter values (Table 1), this time scale is $T = 1/\tau = 10$ days. The dynamics of this no-life fixed point is mainly controlled by the remineralisation process, and logically its associated time scale depends on τ except for very high zooplankton or phytoplankton mortality rates. Moreover τ only defines the time

scale for the system to reach the equilibrium without playing any role in the bifurcation towards other fixed points, according to bifurcation parameters λ_1 and λ_2.

Fixed points n°2 and n°3: They consist of $N^*P_1^*$ and $N^*P_2^*$. Because P_1 and P_2 (with their associated parameters) play symmetric roles in equations 6 to 9, results concerning any of these fixed points can be easily deduced from the other by exchanging subscripts 1 and 2. This is why we only analyse fixed point n°2 : $N^*P_1^*$ (supposing that P_1 outclasses P_2, that is to say $\lambda_1 = \alpha_1 \frac{C_0}{K_{N1}+C_0} - m_p$ becomes positive first). In that case the equilibrium point reached by the dynamical system is the following:

$$N^* = \frac{K_{N1} m_p}{\alpha_1 - m_p} \tag{A.1}$$

$$P_1^* = \frac{\tau}{m_p + \tau}(C_0 - N^*) \tag{A.2}$$

This fixed point exists if and only if $C_0 > \frac{K_{N1} m_p}{\alpha_1 - m_p}$.

The Jacobian matrix eigenvalues at this equilibrium are:

$$\lambda_5 = g\beta \frac{P_1^*}{K_Z + P_1^*} - \varepsilon,$$

$$\lambda_6 = \alpha_2 \frac{N^*}{K_{N2} + N^*} - m_p,$$

$$\lambda_7 = -\frac{\tau + A_1}{2} + \sqrt{\left(\frac{\tau + A_1}{2}\right)^2 - A_1(m_p + \tau)},$$

$$\lambda_8 = -\frac{\tau + A_1}{2} - \sqrt{\left(\frac{\tau + A_1}{2}\right)^2 - A_1(m_p + \tau)}$$

With $A_1 = \alpha_1 \frac{K_{N1}}{(K_{N1}+N^*)^2}$

λ_5 and λ_6 are the bifurcation parameters (they are real and are likely to change

sign) unlike λ_7 and λ_8 whose real part is always negative. λ_5 is responsible for the transition to fixed point $N^*P_1^*Z^*$ and λ_6 for the transition to fixed point $N^*P_2^*$. λ_5 controls the growth of zooplankton whereas λ_6 manages the competition between phytoplankton species. Contrary to λ_5, bifurcation parameter λ_6 is independent of the total amount of nitrogen in the system (C_0). This means that without zooplankton, only light, and not background nitrogen concentration, controls competition between phytoplanktons.

Let us now study in more detail the sensitivity of these two bifurcation parameters to parameter values. Concerning bifurcation parameter λ_5 we have:

$$sign(\lambda_5) = sign\left((\frac{g\beta}{\varepsilon} - 1)\frac{\tau}{m_p + \tau}(C_0 - \frac{K_{N1}m_p}{\alpha_1 - m_p}) - K_Z\right)$$

If $g\beta/\varepsilon < 1$ the fixed point is always stable (λ_5 is always negative) and the zooplankton is not sufficiently efficient to develop. $g\beta/\varepsilon$ is the ratio between the assimilation rate of zooplankton and its mortality rate and thus represents the efficiency of the zooplankton species. When $g\beta/\varepsilon > 1$ the fixed point can destabilize and then cross the bifurcation towards the $N^*P_1^*Z^*$ fixed point as τ, C_0, I, $g\beta/\varepsilon$ increase or $K_{N\,1}$, $K_{I\ 1}$, K_Z, m_p decrease.

Concerning bifurcation parameter λ_6 we have :

$$sign(\lambda_6) = sign(\frac{K_{N1}}{\alpha_1 - m_p} - \frac{K_{N2}}{\alpha_2 - m_p})$$

It shows that fixed point $N^*P_1^*$ will tend to destabilize more quickly towards $N^*P_2^*$ if parameters K_{N1}, K_{I1} and μ_2 are large and parameters K_{N2}, K_{I2} and μ_1 are small. These parameters define the affinity of each phytoplankton species for light and nutrients and therefore the phytoplankton competitivive-ness according to the surrounding environment (nutrients and light availabil-

ity).

Let us discuss now the time scale T associated to this fixed point. We have $T > 1/\varepsilon$ (according to λ_5) or $T > 1/m_p$ (according to λ_6) or $T < \left(\frac{1}{2}(\tau + \frac{(\alpha_2 - m_p)^2}{\alpha_2 K_{N2}})\right)^{-1}$ (according to λ_8). According to the parameter domain of variation, except for very low values of τ, the e-folding time is given by the real part of λ_8. It can be noticed that, in that case, the intrinsic time scale is independent of light.

Fixed points n°4 and n°5: They correspond to $N^* P_1^* Z^*$ or $N^* P_2^* Z^*$. They appear if eigenvalue λ_5 (with the right choice of subscripts 1 and 2) managing zooplankton development becomes positive. As in the previous paragraph we only analyse fixed point $N^* P_1^* Z^*$. The other one can be deduced easily by interchanging subscripts 1 and 2. Values at equilibrium are the following:

$$N^* = -\frac{a - C_0 + b\alpha_1}{2} + \sqrt{\frac{(a - C_0 + b\alpha_1)^2}{4} - (d - K_{N1} C_0)} \tag{A.3}$$

$$P_1^* = \frac{\varepsilon K_Z}{g\beta - \varepsilon} \tag{A.4}$$

$$Z^* = \frac{\beta}{\varepsilon}\left(\alpha_1 \frac{N^*}{K_{N1} + N^*} - m_p\right) P_1^* \tag{A.5}$$

With, $a = K_{N1} + P_1^*\left(1 - \frac{\beta}{\varepsilon} m_p\right)$, $b = P_1^*\left(\frac{\beta}{\varepsilon} + \frac{1}{\tau}\right)$, $d = P_1^* K_{N1} - \frac{\beta}{\varepsilon} m_p K_{N1} P_1^*$

This fixed point is defined when $d - K_{N1} C_0 \leq 0$ (equivalently $C_0 \geq \frac{\varepsilon K}{g\beta - \varepsilon}(1 - \frac{\beta}{\varepsilon} m_p)$), $\frac{g\beta}{\varepsilon} > 1$ and $N^* \geq \frac{K_{N1} m_p}{\alpha_1 - m_p}$.

The equilibrium value P_1^* only depends on zooplankton parameters: neither parameters that define phytoplankton features nor I and C_0 have an influence on the equilibrium phytoplankton value. It means that as soon as Z develops, it totally controls phytoplankton concentration. The more efficient zooplankton is, that is to say the greater $g\beta/\varepsilon$ is, the lower phytoplankton concentration is at equilibrium. And whatever the phytoplankton efficiency,

zooplankton is going to balance it by eating more or less phytoplankton. The more food zooplankton finds, the more it eats. This is in agreement with the results of Edwards and Brindley (1999) with linear zooplankton mortality. An important implication is that phytoplankton value at the equilibrium is the same whatever species emerges (P_1^* or P_2^*), so that phytoplankton characteristics will only affect zooplankton and nutrient concentrations.

Among the four Jacobian matrix eigenvalues related to this equilibrium, one can easily be obtained analytically:

$$\lambda_9 = \alpha_2 \frac{N^*}{K_{N2} + N^*} - \alpha_1 \frac{N^*}{K_{N1} + N^*}$$

This bifurcation parameter is always real and changes sign as parameters vary. It is clearly related to a bifurcation towards fixed point $N^* P_2^* Z^*$. Thus it governs the competition between phytoplanktons in presence of zooplankton, that is to say the switch between the two phytoplankton species.

The three other eigenvalues are given by the following third degree equation :

$$\begin{aligned} &\lambda^3 + \lambda^2 \left[Z^* (V - W) + U + \tau \right] \\ &\quad + \lambda \left[Z^* \left((U + \tau)(V - W) + UW + \beta V W P_1 \right) + U (m_p + \tau) \right] \\ &\quad + Z^* \beta V \left[(U + \tau) W P_1 + U \tau \right] = 0 \end{aligned}$$

with

$$U = \frac{K_{N1} \alpha_1 P_1^*}{(K_{N1} + N^*)^2} \quad V = \frac{g K_Z}{(K_z + P_1^*)^2} \quad W = \frac{\varepsilon}{\beta P_1^*}$$

whose solutions via Cardan formulae are too complicated to provide a clear interpretation of their analytical form. They are computed numerically from these formulae. The sensitivity of these eigenvalues to parameter variations

will be discussed in the following section. We only mention here that for the default parameter set (Table 1) and all the values of C_0 and I considered here, one of these eigenvalues is responsible for the transition towards fixed point $N^*P_1^*$ while the other two are complex conjugates with a real part that change sign when parameters vary. These last two eigenvalues are thus bifurcation parameters associated with a classical Hopf bifurcation. This bifurcation is characterized by a transition towards a limit cycle with the ecosystem structure NP_1Z when the real part of the eigenvalues becomes positive. Identically, from fixed point n°5, we find the same types of bifurcations, either towards fixed point n°4, or toward fixed point n°3, or towards an NP_2Z limit cycle.

Such self-sustained oscillations are usual in ecosystem models (Huisman and Weissing, 1999; Lima et al., 2002b; Edwards and Brindley, 1999; Edwards, 2001). They still raise numerous questions and debates among ecologists about the existence of such oscillations. But lately, a few publications set forth a different view. First, the deep chlorophyll maximum was shown to commonly develop oscillations in temperate region (Huisman et al., 2006) whereas they are usually considered as stable features. This shows that it is possible to find sustained fluctuations of biogeochemical variables. In addition, McCauley and Murdoch (1987) observed internally-driven cycles in riparian ecosystems. Evidence of marine phytoplankton oscillations (chaos) was also very recently given in the context of a long term laboratory mesocosm experiment with constant external conditions (Benincà et al., 2008). Besides, according to Huisman and Weissing (1999), such oscillations are a potential solution to the paradox of the plankton (Hutchinson, 1961). They may allow coexistence between numerous phytoplankton species with a very limited number of mineral ressources. Last, Koszalka et al. (2007), in a numerical study, showed that oscillations present in 0D are attenuated or somewhat concealed in Eulerian measurements when

they are subject to turbulent ocean dynamics.

B Segregation of the two phytoplankton species

We now study the question of coexistence of the two phytoplankton species, that is to say, ecosystem structures n°6 and n°7 in Table 2. The question is: with such a model, is it possible that the two species stably coexist somewhere in parameter space? First, let us consider the case of fixed points. If we suppose that a fixed point without zooplankton but with $P_1^* \neq 0$ and $P_2^* \neq 0$ simultaneously exists, then equations 7 and 8 give:

$$\alpha_1 \frac{N^*}{K_{N1} + N^*} - m_p = 0 \quad and \quad \alpha_2 \frac{N^*}{K_{N2} + N^*} - m_p = 0$$

which is equivalent to:

$$N^* = \frac{K_{N1} m_p}{\alpha_1 - m_p} = \frac{K_{N2} m_p}{\alpha_2 - m_p}$$

This means that without zooplankton, we can not find a fixed point with a coexistence of P_1 and P_2 except on the curve defined by $\frac{K_{N1}}{\alpha_1 - m_p} - \frac{K_{N2}}{\alpha_2 - m_p} = 0$ which is exactly the bifurcation curve $\lambda_6 = 0$ between equilibria n°2 ($N^* P_1^*$) and n°3 ($N^* P_2^*$). If we define variables $\overline{P} = P_1 + P_2$ and $P' = P_1 - P_2$, defining the symmetric and asymmetric parts of the total phytoplankton, it can be shown that on this bifurcation curve, $\overline{P} = \frac{\tau(C_0 - N^*)}{m_p + \tau}$ whatever the value of P', $|P'| \leq \overline{P}$. Elsewhere each fixed point without zooplankton verifies $P' = \pm \bar{P}$ which means $P_1 = 0$ or $P_2 = 0$.

This is consistent with the competitive exclusion principle (Hutchinson, 1961; Passarge and Huisman, 2002) which states that at equilibrium the number of coexisting species can not exceed the number of limiting resources. Here, only variable N is limiting, thus phytoplankton species can not coexist without a predator in the system.

If we suppose now that a fixed point exists with $P_1^* \neq 0$, $P_2^* \neq 0$ and $Z^* \neq 0$, then equations 7 and 8 give:

$$\alpha_1 \frac{N^*}{K_{N1} + N^*} - m_p - g \frac{1}{K_Z + \overline{P}^*} Z^* = 0$$

$$\alpha_2 \frac{N^*}{K_{N2} + N^*} - m_p - g \frac{1}{K_Z + \overline{P}^*} Z^* = 0$$

which implies :

$$\alpha_1 \frac{N^*}{K_{N1} + N^*} - \alpha_2 \frac{N^*}{K_{N2} + N^*} = 0$$

This means that at a fixed point in the presence of zooplankton P_1 and P_2 cannot coexist, except on the bifurcation curve defined by $\lambda_9 = 0$ between the fixed points n°4 ($N^* P_1^* Z^*$) and n°5 ($N^* P_2^* Z^*$). It can be shown that on this bifurcation curve, $\overline{P} = \frac{K_Z \varepsilon}{g\beta - \varepsilon}$ whatever the value of P', $|P'| \leq \overline{P}$. Elsewhere each fixed point without zooplankton verifies $P' = \pm \bar{P}$ which means $P_1 = 0$ or $P_2 = 0$.

The second way for phytoplankton species to coexist at equilibrium is to oscillate. Is it possible for our dynamical system to reach a limit cycle with N, P_1, P_2 or N, P_1, P_2, Z ? First, the limit cycle without zooplankton (NP_1P_2) may appear either from a fixed point or another limit cycle. The first case which comes immediately to mind is a bifurcation from fixed point NP_1P_2 to the corresponding limit cycle. As this fixed point does not exist, this transi-

tion is not possible. The second case is a bifurcation from fixed points $N^*P_i^*$ or $N^*P_i^*Z^*$ to the limit cycle, with $i = 1$ or 2. It is not possible because no eigenvalues of the Jacobian matrix has been found before for such a bifurcation. And the last case would be a transition of the system towards another limit cycle than that considered. This would require a projection of the system on a Poincaré map with determination of the eigenvalues in this new basis. But the calculation is too complex to be solved analytically. Such a transition is, however, unlikely, since in no part of the parameter explored (beyond that presented here) did we find a limit cycle with co-existence of P_1 and P_2. The same reasoning can be conducted for the limit cycle with zooplankton (NP_1P_2Z) to attain the same conclusions.